TP 13921E

PERFORMANCE MEASURES FROM TRACK GEOMETRY CARS:
A Vehicle Dynamic Response Predictor

Prepared for
Transportation Development Centre
Transport Canada

by
TranSys Research Ltd

November 2002

TranSys Research Ltd
682 Milford Drive
Kingston, ON K7M 6B4

TP 13921E

Performance Measures from Track Geometry Cars:
A Vehicle Dynamic Response Predictor

by

G.W. English, T.W. Moynihan and M.J. Korenberg

TranSys Research Ltd
682 Milford Drive
Kingston, Ontario K7M 6B4

November 2002

This report reflects the views of the authors and not necessarily those of the Transportation Development Centre, the Steering Committee or the sponsoring organizations.

The Transportation Development Centre does not endorse products or manufacturers. Trade or manufacturers' names appear in this report only because they are essential to its objectives.

Note on the units used in this report

Because the established practice within the North American railway industry uses imperial units for the basic measures of distance, speed and track geometry measurements, imperial units are used for those measures in this report. For speed and measurement intervals, which occur frequently throughout the report, equivalent metric units are not shown since they would detract from the flow of the text. A table of metric conversions for the units involved is presented below.

In the area of dynamic modelling of vehicle response, the use of metric units is standard practice; therefore, metric units are used for this in the report, with imperial equivalents shown where measures such as car weight are involved.

Conversion Factors	
Imperial Unit	Equivalent Metric Unit
1 in.	25.4 mm
1 ft.	0.3048 m
1 mi.	1.6093 km
1 ton	0.907 t
1 lb.	0.4536 kg (mass) 4.45 N (force)
degree curvature	Radius (m) = $\frac{1{,}746.375}{\text{degrees-curvature}}$

Un sommaire français se trouve avant la table des matières.

Transport Canada / Transports Canada

PUBLICATION DATA FORM

1. Transport Canada Publication No.	2. Project No.	3. Recipient's Catalogue No.
TP 13921E	9926-29	

4. Title and Subtitle	5. Publication Date
Performance Measures from Track Geometry Cars: A Vehicle Dynamic Response Predictor	November 2002
	6. Performing Organization Document No.
7. Author(s)	8. Transport Canada File No.
G.W. English, T.W. Moynihan, and M.J. Korenberg	ZCD2450-110
9. Performing Organization Name and Address	10. PWGSC File No.
TranSys Research Ltd. 682 Milford Drive Kingston, Ontario Canada K7M 6B4	MTB-0-00755
	11. PWGSC or Transport Canada Contract No.
	T8200-000511/001/MTB
12. Sponsoring Agency Name and Address	13. Type of Publication and Period Covered
Transportation Development Centre (TDC) 800 René Lévesque Blvd. West Suite 600 Montreal, Quebec H3B 1X9	Final
	14. Project Officer
	S. Vespa

15. Supplementary Notes (Funding programs, titles of related publications, etc.)

Co-sponsored by Canadian National Railway and Canadian Pacific Railway

16. Abstract

This report presents the results of a 12-month test and analysis program aimed at developing better performance indicators for track geometry. The test program involved the instrumentation of two freight cars to record events of undesirable suspension unloading and the associated track geometry at those locations. The analytic program involved the development of a predictor software program that can be run on board the geometry car to predict where the occurrences of undesirable vehicle response will occur.

The predictor performed well in isolating track conditions that will produce significant vehicle response. In comparison with existing regulatory definitions of track geometry defects, the predictor model had a higher ratio of hit-site identification to false-positives. The findings raised questions of what level of vehicle response should be considered undesirable and what conditions actually pose a derailment risk.

17. Key Words	18. Distribution Statement
Performance measures, track geometry, vehicle dynamics, maintenance planning, unloading, derailment, predictor software	Limited number of copies available from the Transportation Development Centre

19. Security Classification (of this publication)	20. Security Classification (of this page)	21. Declassification (date)	22. No. of Pages	23. Price
Unclassified	Unclassified	—	xiv, 54, apps	Shipping/ Handling

Transports Canada Transport Canada

FORMULE DE DONNÉES POUR PUBLICATION

1. N° de la publication de Transports Canada	2. N° de l'étude	3. N° de catalogue du destinataire
TP 13921E	9926-29	

4. Titre et sous-titre	5. Date de la publication
Performance Measures from Track Geometry Cars: A Vehicle Dynamic Response Predictor	Novembre 2002
	6. N° de document de l'organisme exécutant

7. Auteur(s)	8. N° de dossier - Transports Canada
G.W. English, T.W. Moynihan, et M.J. Korenberg	ZCD2450-110

9. Nom et adresse de l'organisme exécutant	10. N° de dossier - TPSGC
TranSys Research Ltd. 682 Milford Drive Kingston, Ontario Canada K7M 6B4	MTB-0-00755
	11. N° de contrat - TPSGC ou Transports Canada
	T8200-000511/001/MTB

12. Nom et adresse de l'organisme parrain	13. Genre de publication et période visée
Centre de développement des transports (CDT) 800, boul. René-Lévesque Ouest Bureau 600 Montréal (Québec) H3B 1X9	Final
	14. Agent de projet
	S. Vespa

15. Remarques additionnelles (programmes de financement, titres de publications connexes, etc.)

Coparrainé par le Canadien National et le Canadien Pacifique

16. Résumé

Ce rapport présente les résultats d'un programme d'analyses et d'essais qui a duré 12 mois et dont l'objectif était de mettre au point de meilleurs indicateurs de la qualité géométrique de la voie. Le programme d'essais a d'abord consisté à instrumenter deux wagons de marchandises afin de détecter les pertes de contact roue-rail (déchargements) indésirables et les conditions de voie associées à ces déchargements. Le programme d'analyses a comporté le développement d'un logiciel de prédiction conçu pour être exploité à bord de la voiture de contrôle et détecter les endroits où des réactions indésirables du véhicule doivent être attendues.

L'algorithme de prédiction s'est révélé utile pour détecter les conditions de voie engendrant de fortes réactions des véhicules. Si on compare le nombre de sites problèmes définis à partir des critères réglementaires en vigueur et le nombre de sites détectés par l'algorithme, on constate que ce dernier conduit à un rapport supérieur du nombre de détections au nombre de faux positifs. Ces résultats ont mené les chercheurs à se poser les questions suivantes : à partir de quel point les réactions des véhicules doivent-elles être considérées comme indésirables et dans quelles conditions les véhicules sont-ils réellement exposés à un risque de déraillement?

17. Mots clés	18. Diffusion
Mesure de la qualité de la voie, géométrie de la voie, dynamique des véhicules, planification de l'entretien, déchargement, déraillement, logiciel de prédiction	Le Centre de développement des transports dispose d'un nombre limité d'exemplaires.

19. Classification de sécurité (de cette publication)	20. Classification de sécurité (de cette page)	21. Déclassification (date)	22. Nombre de pages	23. Prix
Non classifiée	Non classifiée	—	xiv, 54, ann.	Port et manutention

Acknowledgements

The authors would like to thank the project steering committee members for feedback and support of this project:

- Sesto Vespa and Ling Suen, Transport Canada's Transportation Development Centre
- Jovite Grondin and George Achakji, Transport Canada's Rail Safety Directorate
- Nigel Peters and William Blevins, Canadian National Railway
- Michael Roney, Canadian Pacific Railway

The authors would like to thank all of the personnel associated with CPR's Track Evaluation Car and CN's TEST car for their cooperation and assistance during test data collection. We would also like to thank Procor Ltd and CPR for the loan of a tank car and hopper car, respectively, for the duration of the tests. The project evolution was significantly influenced by input from associates who contributed to the project at different stages but who were not involved in the final report. Dr. Ron Anderson, Professor of Mechanical Engineering at Queen's University provided advice on—and use of—his vehicle dynamic software package A'GEM. We also thank Jerry Slaba of NDT Technologies, whose firm provided instrumentation support for the test phase.

Executive Summary

Instrumentation and data acquisition systems were developed for each of Canadian National Railway's (CN) and Canadian Pacific Railway's (CPR) geometry cars to collect geometry and test car dynamic response data. Vertical spring-nest displacements were measured for the four suspensions of two test cars. A tank car and a hopper car were identified as cars with a higher derailment risk from geometry conditions. An empty tank car and an empty hopper car were instrumented and transported across CN's and CPR's rail networks coupled with the respective railway's track geometry car. The geometry cars provide speed, curvature, location and the geometric conditions that the test cars are traversing. Threshold displacements were selected to denote undesirable levels of suspension unloading. When these thresholds were exceeded, dynamic data were recorded and later retrieved from the geometry car and evaluated. This instrumentation met the project's first objective of providing a low-cost means of detecting when and where high dynamic action occurred. The low-cost instrumentation allowed a broad coverage of Canada's railroad network and provided insight into what geometry conditions lead to high dynamic response for the two empty car types that were tested.

The car response data from the two railways' systems were then assessed with the objective of developing a "bad-spot" detector software algorithm that would consider all geometry information to determine those combinations of parameters and car type/speed that lead to an undesirable level of suspension unloading. The work to date has been successful in identifying locations of high dynamic action and developing the ability to predict them. This partially met the second project objective, which was to predict locations that would stimulate undesirable vehicle response; however, as discussed below, there is no clear definition of what level of dynamic action is "undesirable" to the point of being a derailment risk.

Similarly, the third objective of identifying inappropriate response of a specified car was partially met, but lacks a clear definition of "inappropriate". Track conditions that produce high dynamic action can be predicted for the specific cars tested, but the number of occurrences for the initial definition of "inappropriate" is too high to be economically applied as a "corrective-action-required" indicator. The predictor software identifies many more sites than the existing regulatory defect criteria for lower class tracks. Nonetheless, vehicle dynamic action and suspension unloading are necessary ingredients for geometry-related derailments and the existing regulatory measures were not well correlated with the measured "hit" sites. The predictor that has been developed is a good measure of track performance, but it requires more detailed insight into wheel forces to select a reasonable threshold (i.e. a better definition of "undesirable" unloading).

Sommaire

Une instrumentation et des systèmes de collecte de données ont été mis au point pour chacun des wagons d'analyse de la géométrie de la voie du Canadien National (CN) et du Canadien Pacifique (CP), afin d'étudier la géométrie de la voie et les réactions dynamiques de wagons d'essai. Le déplacement vertical des blocs-ressorts des quatre suspensions de deux wagons d'essai a été mesuré. Il a ainsi été déterminé que les wagons-citernes et les wagons-trémies sont les types de wagons qui risquent le plus de dérailler en cas de défaut de géométrie de la voie. Un wagon-citerne vide et un wagon-trémie vide ont été instrumentés et chacun a été jumelé au wagon d'analyse de la géométrie de la voie de l'un et l'autre chemin de fer. Ils ont ensuite parcouru les réseaux du CN et du CP. En plus des données sur la géométrie de la voie dans les zones traversées, les wagons d'analyse fournissent des renseignements sur la vitesse, la courbure de la voie et l'emplacement. Des valeurs seuils de déplacement des blocs-ressorts ont été déterminées en fonction de pertes de contact roue-rail indésirables (déchargements). À chaque fois que ces seuils étaient dépassés, les données dynamiques étaient enregistrées et extraites plus tard, pour analyse. Cette instrumentation constituait un moyen de recenser à peu de frais quand et où étaient déclenchées des réactions dynamiques significatives. Le premier objectif assigné au projet a donc été atteint. Cette instrumentation peu coûteuse a permis de couvrir une vaste portion du réseau ferroviaire canadien et de mieux connaître les états géométriques menant à de fortes réactions dynamiques dans les deux types de wagons vides étudiés.

Les données sur les réactions des wagons des deux chemins de fer ont ensuite servi à développer un algorithme de détection des «sites problèmes». L'algorithme prend en compte toutes les données sur la géométrie de la voie et détermine quelles combinaisons de paramètres et de type/vitesse de wagon conduisent à un degré indésirable de déchargement. Les travaux réalisés à ce jour ont permis de recenser les sites où se déclenchent de fortes réactions dynamiques et de développer un logiciel pour prédire ces sites. Le deuxième objectif assigné au projet, celui de déterminer les endroits propices au déclenchement de réactions indésirables dans les véhicules, a ainsi été partiellement atteint; toutefois, comme on le verra ci-après, il n'existe pas de définition claire du degré de réaction «indésirable» pouvant être assimilé à un risque de déraillement.

De même, le troisième objectif, soit celui de déterminer ce qu'est une réaction inappropriée dans un wagon donné, a été partiellement atteint, mais il reste encore à définir clairement ce qu'est une réaction «inappropriée». La méthode permet de prédire les conditions de voie qui engendrent de fortes réactions dynamiques dans les wagons précis mis à l'essai. Toutefois, le nombre de cas de déchargements nécessaires pour définir un site comme «inapproprié» est trop élevé pour que la méthode puisse constituer

un indicateur efficace de la nécessité d'une intervention. Le logiciel de prédiction détecte beaucoup plus de sites problèmes que ne le prévoient les critères réglementaires actuellement utilisés pour définir comme défectueuses les voies de catégorie inférieure. Pourtant, les réactions dynamiques des véhicules et les pertes de contact roue-rail sont les facteurs essentiels des déraillements attribuables aux défauts de géométrie de la voie, et l'étude n'a pas permis d'établir une corrélation significative entre, d'une part, les «sites problèmes» définis à la lumière du règlement en vigueur, et, d'autre part, les sites détectés par le logiciel développé dans le cadre du projet. Ce logiciel s'avère satisfaisant pour mesurer la qualité de la voie, mais il faudra approfondir la question des forces au contact rail-roues pour pouvoir établir un seuil raisonnable de déchargement (c.-à-d. définir précisément ce qu'est un déchargement «indésirable»).

Table of Contents

1 INTRODUCTION 1

1.1 BACKGROUND 1
1.2 OBJECTIVES 2
1.3 REPORT LAYOUT AND CONTENT OF SUBSEQUENT CHAPTERS 3

2 TEST CARS AND DATA ACQUISITION 4

2.1 TEST CARS 4
2.2 INSTRUMENTATION AND DATA ACQUISITION 6
2.2.1 CN TEST Consist 8
2.2.2 CPR TEC Consist 8
2.3 UNLOADING CRITERIA 9
2.3.1 AAR Chapter Eleven 9
2.3.2 Estimated Wheel Unloading 10
2.3.3 Estimated L/V Ratio 10

3 PREDICTOR SOFTWARE DEVELOPMENT 13

3.1 QUASI-LINEAR PHYSICAL MODEL 13
3.1.1 Vehicle Models 14
3.1.2 Response Predictor Program 16
3.2 NON-LINEAR PARAMETRIC MODEL 17

4 OBSERVATIONS FROM THE DATA / PREDICTOR MODEL 18

4.1 CURVATURE INFLUENCE 18
4.2 VEHICLE INFLUENCE 22
4.3 SPEED INFLUENCE 24
4.4 TRACK CLASS INFLUENCE 27
4.4.1 Example of High-Speed Response 27
4.4.2 Example of Low- and Medium-Speed Response 28

5 RELEVANCE TO REGULATORY DEFECTS/EXCEPTIONS 31

5.1 COMPARISON OF PREDICTIVE ACCURACY 31
5.1.1 Class 4 Prairie Subdivision - Hopper Car 32
5.1.2 Class 3 Mountain Subdivision - Hopper Car 33
5.1.3 Class 3 and 4 Mountain Subdivision - Tank Car 34
5.1.4 Class 4 Canadian Shield Subdivision - Hopper Car 35
5.1.5 Mixed Class 2 and 3 Subdivision - Hopper Car 37
5.2 INSIGHT INTO SPECIFIC REGULATORY DEFECTS 38
5.2.1 Unbalanced Superelevation Influence 38
5.2.2 Combined Priority Defects 40

6 PREDICTOR IMPLEMENTATION 44

6.1 MODEL ATTRIBUTES 44
6.2 INDEX VERSUS DEFECT INTERPRETATION 44
6.3 FIXED OR VARIABLE THRESHOLD 49

6.4 APPLICATION NOTES 49
7 CONCLUSIONS AND RECOMMENDATIONS 51
7.1 CONCLUSIONS 51
7.2 RECOMMENDATIONS 51

REFEERENCES 53

APPENDIX A Instrumentation

APPENDIX B Parallel-Cascade Methodology

List of Figures

Figure 1 Photograph of tank car PROX 83806 5
Figure 2 Photograph of hopper car CP 388545 5
Figure 3 Test car instrumentation 6
Figure 4 Data acquisition system 7
Figure 5 Simulation of wheel and suspension unloading relationship 11
Figure 6 Unloading threshold characteristic 12
Figure 7 Example surface and cross-level transfer functions 15
Figure 8 Illustration of parallel-cascade prediction accuracy 17
Figure 9 First illustration of curve dampened response 19
Figure 10 Second illustration of curve dampened response 20
Figure 11 Illustration of a curve with a high prediction error 21
Figure 12 Frequency of unloading on the high rail side in curves 23
Figure 13 Predicted hit frequency versus train speed (Class 2 track, jointed rail) 24
Figure 14 Effect of 10 mph speed limit on the hopper car 25
Figure 15 Effect of 10 mph speed limit on the tank car 26
Figure 16 Distribution of unloading incidents versus train speed 26
Figure 17 Hopper car hits, Class 4 track 28
Figure 18 Hopper car hits, mixed Class 2 and 3 track 29
Figure 19 Predicted, actual and regulatory defects, Class 4 track 32
Figure 20 Predicted, actual and regulatory defects, Class 3 mountain subdivision 34
Figure 21 Predicted, actual and regulatory defects, Class 3 and 4 mountain subdivision 35
Figure 22 Predicted, actual and regulatory defects, Class 4 N. Ontario subdivision 36
Figure 23 Unbalanced superelevation in tangent track 38
Figure 24 Unbalanced superelevation in very low curvature 39
Figure 25 Car dynamics at a multiple priority defect 41
Figure 26 Suspension lift-off at a single priority-defect site 43
Figure 27 Comparison of measured bounce hits with track roughness 45
Figure 28 Comparison of predictor with measured bounce dynamics 45
Figure 29 Index interpretation of predictor output on Class 2 track 46
Figure 30 Local defect interpretation of predictor output on Class 3 and 4 track 48

List of Tables

Table 1 Principal characteristics of the test cars 4
Table 2 Data acquired on the test consists 7
Table 3 Comparison of tank car and hopper car hit frequency 23
Table 4 Number of hits versus unloading threshold, Class 4 track 27
Table 5 Number of hits versus unloading threshold, Class 2 and 3 track 29
Table 6 Predictor/regulation comparison, Class 4 track 33
Table 7 Predictor/regulation comparison, Class 3 mountain subdivision 33
Table 8 Predictor/regulation effectiveness, Class 4 N. Ontario 37
Table 9 Comparison of hit and defect frequency, Class 2 and 3 track 37

Glossary of Acronyms

AAR	Association of American Railroads
A/D	analogue-to-digital
CNR	Canadian National Railway
CPR	Canadian Pacific Railway
CPU	central processing unit
DSP	digital signal processor
FFT	fast Fourier transform
FRA	Federal Railroad Administration
GPS	global positioning system
LCR	lower centre roll
L/V	lateral-to-vertical
MCO	mid-chord offset
PC	parallel cascade
PSD	power spectral density
RC	rate of change
SE	superelevation
TEC	track evaluation car
RMS	root mean square

1 INTRODUCTION

1.1 Background

The principal means deployed by all major railways in measuring the geometric quality of track is a track geometry car or track evaluation vehicle. While these vehicles have the capability of measuring track parameters of interest, the interpretation of the measurements in assessing track condition and in deciding what to do about it varies widely and is in continuous evolution.

Most railways process their track geometry measurements on a short-segment basis in an effort to assess the overall level of quality. The processing provides a Track Quality Index, which is then used to trigger maintenance action at specified thresholds. The variances (or standard deviations) of geometry deviations are indices used by many railways as surrogates for quality. Variance provides a valid indication of track geometry "roughness"; however, it has limitations as a performance measure, the principal one being that vehicle dynamic response is very dependent on the wavelength of track deviation stimuli. Thus, a relatively smooth track segment at a critical wavelength may produce a more violent vehicle response than a rougher segment at a different wavelength.

Regulatory defects (or exceptions) are also derived from the track evaluation cars. These are local geometric conditions with thresholds—defined within the Canadian Track Standard Regulations—that trigger immediate slow orders until maintenance action is taken. Defect definitions have evolved on a historic basis of judgement and derailment experience. The uncertainty in their effectiveness is highlighted by the Canadian railways' experience of significant increase in defect count on well-performing track when they incorporated Federal Railroad Administration (FRA) track standards into their own standards in 1992 [Roney, 1993].

A key factor in the present track geometry regulations is that they focus largely on single track perturbations and involve a measurement system that is forced to meet physical verification via measurement of mid-chord offset (MCO) from a 62 ft. chord. Track-vehicle dynamic interaction is speed dependent and can be influenced more by a series of small deviations at a critical wavelength than a single large perturbation. This has been known to the industry for some time and the authors have been involved in a number of test/development programs addressing the issue.

In 1987, the Association of American Railroads (AAR) conducted a series of truck component loading investigations involving a strain-gauged bolster on a 70 ton boxcar.

The bolster load was monitored and excess loads triggered a paint sprayer to mark track locations of high loads. These tests identified several locations where design loads were exceeded in normal revenue service trains. Follow-up investigations of track geometry data recordings at the locations of high loads revealed that the geometry car's defect criteria identified no particular problems at these locations. The geometry at all locations conformed to the applicable FRA track classification.

The present study follows a previous attempt by the authors to develop a wheel load prediction algorithm [TranSys Research, 1997]. Tests were conducted on a 100 mi. track segment with a 100 ton instrumented wheel set coupled to Canadian Pacific Railway's (CPR's) track evaluation car (TEC). That study noted two particular limitations to accurately predicting vehicle response to track geometry data. The first was a data problem related to the 62 ft. MCO recording used by the CPR geometry car at the time of the study. The measure distorted the true profile and totally eliminated some key wavelengths. The second limitation was primarily a modelling one. The model used in the study was developed for a response to vertical inputs only. Those areas of significant difference between model and field data for roll response were found to be due to lateral forces. To overcome this limitation would require a model enhancement to accept lateral stimulus and a separate lateral model to predict the occurrence of major dynamic lateral forces. A final non-technical problem was that the use of an instrumented wheel set in those tests limited the scope (from cost considerations) to a short track segment. Without prior knowledge of what to expect, the data acquired did not exhibit any significant dynamic action.

Each of the above problems has been addressed in the present study. Canadian National Railway's (CN's) geometry car uses inertial measurements in all but curvature and since the last test program, CPR has retrofitted its TEC with inertial measurement systems on all parameters. A lateral input has been developed as part of the present project's predictor software development, and the instrumentation devised for the test program provides an economical means of undertaking a broad sweep of the total track network to find sites of high dynamic response.

1.2 Objectives

The objective of this project is to reduce train derailments, including some termed "unexplained", by lowering the incidence of undesirable track-vehicle dynamics and by:

1. Providing a low-cost means to detect and advise when and where undesirable levels of wheel unloading occur,

2. Providing the means for geometry cars to detect undesirable sites on an ongoing basis, and

3. Identifying track locations giving rise to inappropriate vehicle response for a specified car type.

1.3 Report Layout and Content of Subsequent Chapters

The balance of this report is divided into six chapters. In Chapter 2 we describe the instrumentation, data collection activity and criteria for denoting undesirable levels of vehicle response.

In Chapter 3 we describe the development of predictor software for on-board processing of track geometry data and in Chapter 4 we present our observations of the data collected and application of the predictor software.

In Chapter 5 we assess the performance of the predictor relative to that of the existing definitions of regulatory defects/exceptions and in Chapter 6 we discuss the implications of the findings for the application of the predictor software.

Finally, in Chapter 7 we present our conclusions and recommendations.

2 TEST CARS AND DATA ACQUISITION

In this chapter we describe the freight cars that were selected for testing and the instrumentation installed on each test car.

2.1 Test Cars

The steering committee identified two car types that exhibited a higher than average derailment frequency from track geometry causes. One was an empty tank car with truck centre spacing of 16.458 m (54 ft.); the other was an empty hopper car with truck centre spacing of 14.07 m (46 ft.). The principal characteristics of the two cars are presented in Table 1.

Table 1 Principal characteristics of the test cars

Description	Units	Tank Car	Hopper Car
Total Mass	kg	39,500	29,091
Sprung Mass	kg	32,024	21,615
Suspension Stiffness (per spring nest)	kN/m	4,596	4,796
Static Spring Deflection	mm	17.1	11.0
Axle Spacing	m	1.778	1.778
Truck Spacing	m	16.458	14.07

The tank car used in the tests (PROX 83806) is pictured in Figure 1 and the hopper car (CP 388545) is pictured in Figure 2. The test cars were coupled forward of the track geometry measurement cars operated by CPR and CN in their normal track evaluation service over a period of 12 months.

Figure 1 Photograph of tank car PROX 83806

Figure 2 Photograph of hopper car CP 388545

2.2 Instrumentation and Data Acquisition

The instrumentation package carried on each instrumented rail vehicle included four linear displacement transducers and two bi-axial accelerometers.[1] See Appendix A for a list of instrumentation. The instrumentation schematic is illustrated in Figure 3.

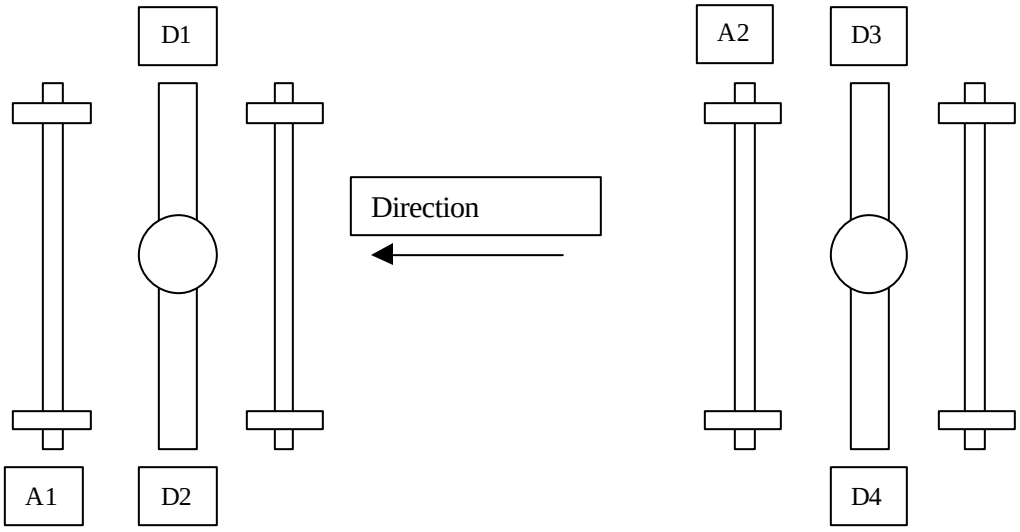

Legend:

A1	Accelerometer (on side frame over lead left wheel)
D1, D2	Displacement Transducers (across each spring nest)
A2	Accelerometer (on side frame over lead right wheel)
D3, D4	Displacement Transducers (across each spring nest)

Figure 3 Test car instrumentation

A schematic of the data acquisition system and interface electronics installed on the CN TEST car and the CPR TEC car 64 is presented in Figure 4. The power and signals are carried from the track geometry vehicle via a multi-conductor shielded cable passing through the floor and running along the exterior of all vehicles coupled between the track geometry car and the instrumented car. The power and signal cable connects to a weatherproof junction box mounted at the rear of the instrumented vehicle using a military style weatherproof connector, while the cabling to individual instruments on a car are fed into the junction box through weatherproof cable seals. The instrumentation package carried on the tank and hopper cars was designed to be electrically

[1] The accelerometers were included in the original test plan to provide a means of determining wheel set motion. As the final test program involved data collection in concert with railway track geometry cars that provided a direct measure of the rail perturbations, the accelerometer data were of limited use. Once the data from the geometry measurement car and the instrumented freight cars were aligned, the accelerometer data were no longer used.

interchangeable so that either instrumented car could be carried along with either the CPR or CN track geometry measurement consist.

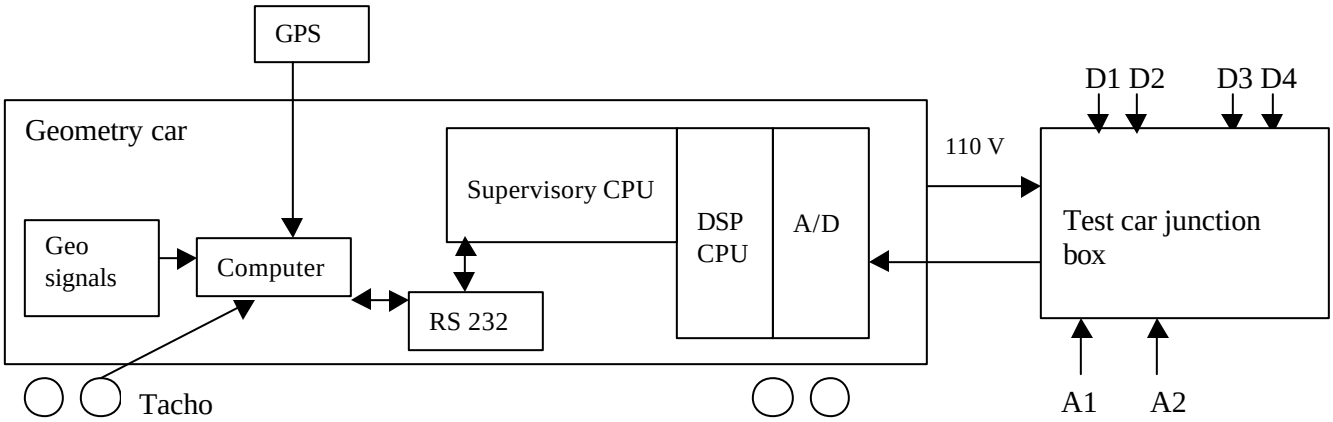

Figure 4 Data acquisition system

A data acquisition system and interface electronics package was installed on both the CN TEST car and the CPR TEC car 64, and was operated by the respective car staffs independently of the other on-board equipment. Table 2 summarizes the data collected. Post-processing of the data was required to align each of the track geometry signals with the instrumented tank/hopper car signals.

Table 2 Data acquired on the test consists

Channel	Signal Description	Scale
0	Track left rail vertical profile	0.250 in/V
1	Track right rail vertical profile	0.250 in/V
2	Left rail alignment	1.000 in/V
3	Right rail alignment	1.000 in/V
4	Track gauge	0.250 in/V
5	Track superelevation	2.000 in/V
6	Track curvature	2.000 deg/V
7	Test train speed	10.00 mph/V
8	Leading truck left spring nest (test car)	0.628773 in/V
9	Leading truck right spring nest (test car)	0.623752 in/V
10	Trailing truck left spring nest (test car)	0.623752 in/V
11	Trailing truck right spring nest (test car)	0.626253 in/V
12	Left bearing adapter vertical acceleration (test car)	0.566 g/V (nominal)
13	Left bearing adapter lateral acceleration (test car)	3.496 g/V (nominal)
14	Right bearing adapter vertical acceleration (test car)	0.566 g/V (nominal)
15	Right bearing adapter lateral acceleration (test car)	3.496 g/V (nominal)

2.2.1 CN TEST Consist

The data acquisition system deployed on CN's TEST car was configured to simultaneously acquire the track geometry signals supplied by the CN TEST car instrumentation and the signals obtained from the transducers mounted on the instrumented tank/hopper cars.

All data were acquired on a continuous basis. The data acquisition system continuously scans and digitizes all signals at a constant time-based frequency and saves these data whenever the train is travelling above a threshold speed (set at 10 mph). A scan rate of 180 Hz was initially used and subsequently reduced to 90 Hz to ease the processing load. The system also detects (at the full continuous scan rate) threshold levels of the spring nest deflection signals and maintains a log of significant secondary suspension unloading events.

The data acquisition system tracks location independently of the CN TEST car's on-board computer from a starting location supplied by the operator at system start up using a nominal 1 ft. pulse train and direction signal. The pulse train is fed into a 16-bit Intel 8254 programmable interval timer whose counter is latched and read on every scan cycle, and the location is suitably updated to the nearest nominal 1 ft. interval. A self-contained Garmin GPS system, model GPS35-LVS, was mounted on top of the CN TEST car and connected to the data acquisition system via an RS-232 port. This unit provides the current car latitude and longitude to the data acquisition system continuously at one-second intervals, whenever there is sufficient satellite reception. The data acquisition system uses this information to log car locations at 0.1 mi. intervals, wherever the centre infrared detector triggers and whenever a manual milepost reset occurs. This provides a backup means of locating collected data in cases where the data acquisition system position is poorly aligned with the actual track mileage.

2.2.2 CPR TEC Consist

The CPR system was configured to monitor instrumented car signals at a constant time-based scan frequency and only saved data to binary disk files around locations where significant suspension unloading events were detected. The system tracks location independently of the CPR TEC car's on-board computers from a starting location supplied by the operator at system start up using a tachometer pulse train and direction signal. A log file is maintained to record the location, file name and severity whenever a threshold event is triggered.

Because of technical limitations restricting the interface to the TEC car's on-board computers, it was not possible to gain real-time access to the track geometry signals.

Rather, the complete track geometry was supplied (in the form of a special "one-foot" file) from the TEC computer at the end of a test. These data have been suitably processed such that all track geometry measures are aligned to correspond with the same spatial location on the track.

2.3 Unloading Criteria

At the beginning of the tests we did not know what to expect in terms of vehicle dynamic activity. Thresholds were set low enough to trigger data collection for analyses. The specific thresholds that were set in the analyses of the data presented in this report were tied to surrogates of "undesirable" vehicle response.

2.3.1 AAR Chapter Eleven

Chapter eleven of the AAR Manual of Standards and Recommended Practices [AAR, 1993] presents a criterion for dynamic response to track irregularities by which new rail cars are certified. The evaluation of new car designs involves an assessment of car response to a perturbed test track.[2] Car response is measured with fully instrumented wheel sets. The instrumented wheel sets provide an indication of both the lateral and vertical forces at the wheel and thus allow for the determination of a lateral-to-vertical (L/V) force ratio.

The "roll" test is conducted under both empty and fully loaded conditions, while the "bounce" test is conducted at a fully loaded state. For a car to be certified, it must not exceed the following limits for a period greater than 50 msec:

- a minimum vertical load of 10 percent of the static load (bounce/pitch or roll)
- a maximum L/V of 1.0 (roll/twist)

The project steering committee further suggested that a limit of 80 percent unloading at the wheel had been found through vehicle simulations of previous derailments to be undesirable in some circumstances. We note that these threshold levels can be designated as "undesirable" response levels but do not necessarily predict a state of imminent derailment. For example, the L/V ratio used in Chapter 11 of [AAR, 1993] is below the commonly accepted formula for wheel climb derailments developed by Nadal.

---

[2] The test track perturbations involve track characteristic of jointed rail settlement (a rectified sine wave with a 39 ft. period). The "roll" test track presents a 3/4 in. variation with left and right side rail joints offset by 18.5 ft., while the "bounce" test presents a 3/4 in. variation with left and right side rail joints coinciding at the same locations.

Nadal's formula considers the force ratio required at the flange-rail interface to sustain wheel climb after tread lift-off. The formula defines the threshold of acceptable ratio of L/V force at the flange interface.

$$L/V \leq (\tan a - u) \Big/ (1 + u \tan a)$$

Where:
L = lateral wheel flange force
V = vertical wheel flange force
α = the flange contact angle
υ = the flange-rail friction coefficient

The formula leads to critical L/V ratios in the order of 1.4 for non-lubricated rail conditions and ratios of 2.0 and higher for a lubricated gauge face condition.

2.3.2 Estimated Wheel Unloading

We note that the above threshold values are specified in accordance with measurement of forces occurring at the wheel. We need to have a basis to relate these thresholds at the wheel to our test measurements of vertical unloading at the car's suspension. Lacking measured data to correlate suspension activity with wheel load forces, we conducted detailed non-linear time-domain simulations of an empty vehicle to relate the two. The simulation results indicate that the force variation at the wheel is more extreme than the variation at the suspension. The top chart in Figure 5 illustrates suspension displacements occasionally dipping to 35 percent of static values (or 65 percent unloading). The bottom chart of Figure 5 illustrates that the relative load at the wheels is at about 20 percent (or 80 percent unloading). On the basis of the simulation results, we set a threshold of 67 percent suspension unloading to reflect the possibility of 80 percent wheel unloading.

2.3.3 Estimated L/V Ratio

In addition to the estimated relationship between vertical wheel force and the force at the suspension discussed above, one can estimate the lateral force that is present in curves.

The wheel climb condition is more relevant for vehicle roll response situations where the vertical load is shifted to the opposite wheel and still produces a lateral force from the tread creep forces. In a bounce response, both wheels are unloaded and the lateral force is reduced proportionately to the vertical unloading. Thus, the L/V condition is only applied to roll response in curves.

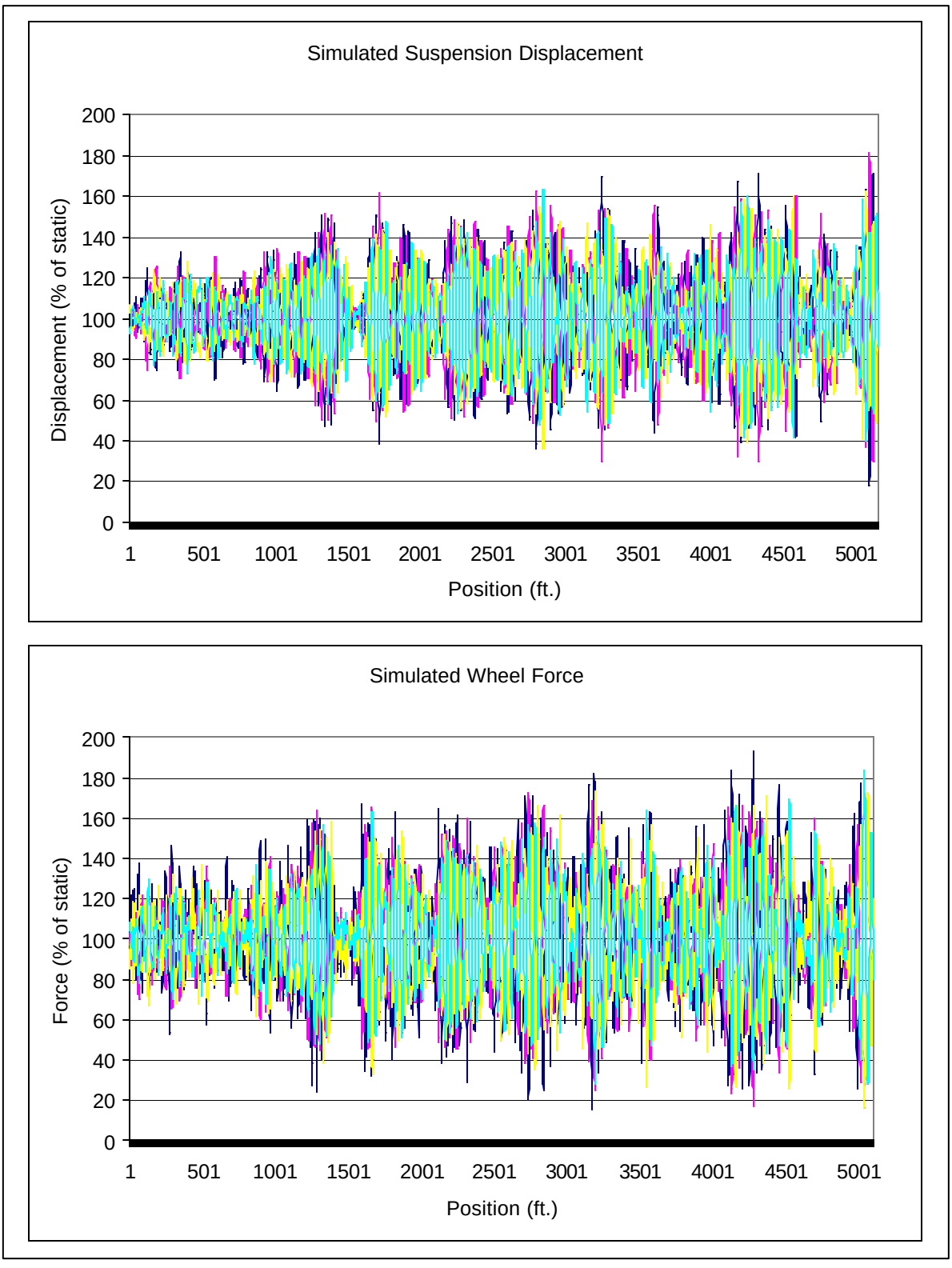

Figure 5 Simulation of wheel and suspension unloading relationship

The lateral flange force (and thus the L/V ratio) increases with increasing curvature. However, the L/V threshold is dependent on several key variables, most of which are controlled such that the impact is mitigated with increasing curvature. The track gauge is increased in curves to allow the wheel conicity to contribute more to curve negotiation. Also, as noted previously, wheel flange or gauge face lubrication significantly elevates the L/V threshold. Since more intense curves on main lines are more likely to have lubricators, the threshold will not increase linearly with curvature. Lacking detailed measurement of the wheel rail forces, we allow for an increasing lateral force with increasing curvature but not on a one-to-one basis. The threshold characteristics adopted for inclusion and for priority-designation in the predictor model are illustrated in Figure 6.

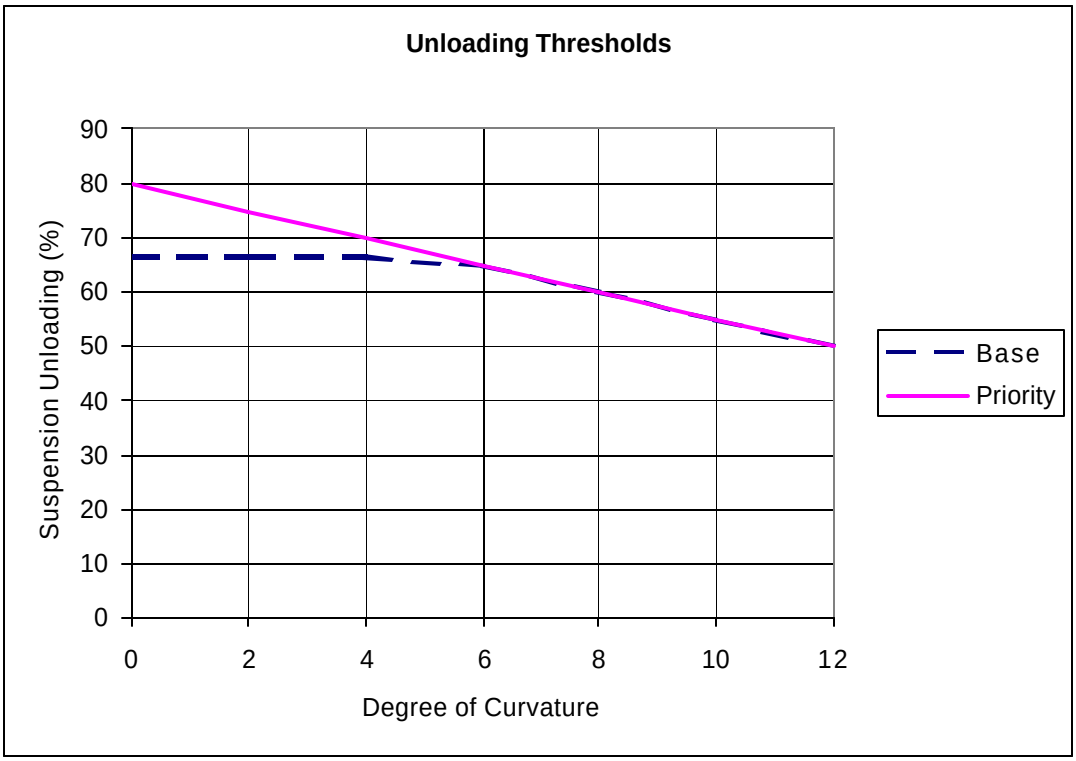

Figure 6 Unloading threshold characteristic

3 PREDICTOR SOFTWARE DEVELOPMENT

Two predictors were assessed—a linear model based on the physical characteristics of the test cars and a non-linear parametric model. Each type of model has advantages and disadvantages. While the railway cars are known to have many non-linearities, the linear models offer significant advantages in providing insight into the nature of response at hit sites and offer the promise of a mechanism to extend the predictive capability to other car types without requiring extensive data collection.

As we show in Section 3.1, the linear model provides a good predictive capability at train speeds that stimulate the dominant dynamic response modes. It was less accurate in predicting hits that occurred at intermediate speeds; however, the sites predicted at the critical speeds tended to encompass those sites that occurred at other speeds.

3.1 Quasi-Linear Physical Model

Linear frequency-domain models of the rail vehicles were developed to predict response to track geometry. In this technique the model relates the wheel set vertical and roll degrees of freedom to the excitation of track geometric (surface, cross-level and alignment) variation. Root mean square (RMS) values of the total resulting force and moment acting on each wheel set are predicted for the power spectral density (PSD) representation of the track geometry.

The response models were initially developed from physical characteristics of the test cars. The starting point for the linear models was the suite of analysis tools provided with the A'GEM Rail Vehicle Dynamics Software Package[3] developed by Dr. Ronald. J. Anderson of Queen's University at Kingston [Kortum, 1992]. The adoption of a linear vehicle model restricts the suspension element characterization to involve only linear stiffness and viscous damping. This allows all internal forces developed within connection elements to be described in terms of linear relationships with respect to relative motions of the vehicle's assigned degrees of freedom. The characteristics of the transfer functions were then altered and other influencing parameters added to provide a better fit with the unloading events in the collected data.

[3] Within the framework of the A'GEM package, the rail vehicle response predictor program developed for these analyses automatically generates the dynamic equations of motion for a rail vehicle model from a description of its dimensions, the inertial properties of each rigid body in the model, and the force relationships of all elements connecting rigid bodies to one another.

3.1.1 Vehicle Models

The rail vehicle model is comprised of 11 rigid bodies, 35 degrees of freedom and 22 connection elements. The rigid bodies include four axles, four truck side frames, two truck bolsters and a car body. Each of the four wheel sets is assigned vertical and roll (rotation about longitudinal coordinate direction) degrees of freedom and is connected to one end of a truck side frame via tri-directional point elements (having linear stiffness and damping in longitudinal, lateral and vertical coordinate directions but small deflections). Each of the four truck side frames is assigned lateral, vertical and pitch (rotation about lateral coordinate direction) degrees of freedom, is connected to each axle as previously described and is connected to one side of a bolster with a bi-directional (longitudinal and lateral) point element and a vertical directed element (elements with substantial length and deflection). Each bolster is assigned lateral, vertical and roll degrees of freedom, is connected to the side frames as previously described and is connected to the car body with a bi-directional point element (longitudinal and lateral coordinate directions) positioned at the centre pin location and with a pair of unidirectional point elements (vertical coordinate direction) positioned on either side of the centre pin at the edge of the centre plate.

Figure 7 illustrates the relative influence of speed on the magnitude of both the surface (upper plot) and cross-level (lower plot) transfer functions calculated for a sample tank car model. The figure contains separate traces of the response transfer function at speeds of 30 mph, 45 mph and 60 mph plotted against the length of the periodic input stimulus of the track geometry variation. We note that the figure is presented for illustrative purposes only. Because of non-linear response elements in freight cars, the actual models used in the predictor have to be modified from the predictions illustrated in this simple linear model. Nonetheless, the trends are relevant. It can be seen that, to stimulate bounce at 30 mph, significant variation must be present in the track surface over a relatively short track length of six or seven feet. Variations are very unlikely to develop over such a short length of track. Stimulus of bounce at 45 mph is associated with more feasible track variations, but is still narrowly focused at one wavelength (18 ft.). At 60 mph, the vehicle will be stimulated by any track variation with a period in the range of 15 to 30 ft.

The stimulus of vehicle roll response is seen to be much more sensitive to speed. Roll is not stimulated at 60 mph, and the magnitude of response at 30 mph is almost double that at 45 mph.

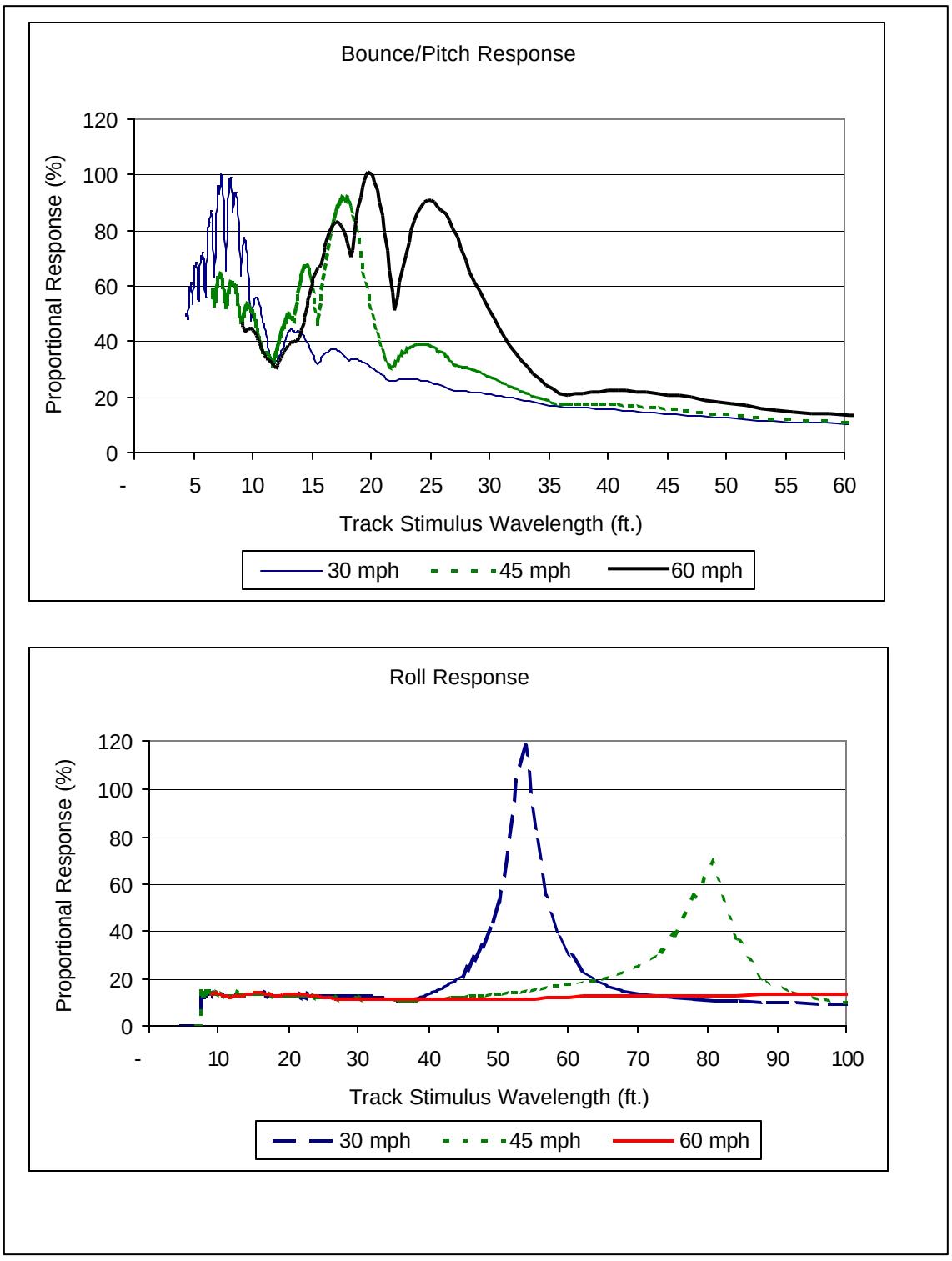

Figure 7 Example surface and cross-level transfer functions

As noted previously, the inclusion of bolster and car body lateral degrees of freedom enables a representation of both lower centre roll (LCR) and upper centre roll motions. The LCR mode, where the centre of car body roll motion is located below the car body's centre of mass, involves a combination of lateral motion of the car body's centre of mass and rotation of the car body, and is typical of rail car rock and roll behaviour. If the lateral car body degree of freedom were not included, the model would be forced to represent car body roll as a simple roll about its centre of mass location. Similarly, the longitudinal car body degree of freedom facilitates realistic car body pitch motion.

3.1.2 Response Predictor Program

The program is designed to automatically window the track data for a user-specified fast Fourier transform (FFT) size and then calculate the equivalent PSD of surface, alignment and cross-level for the target vehicle speed. The track PSD is then applied through the respective transfer functions to yield PSDs of the vehicle response. The predictor then calculates the RMS of wheel set force and moment by integrating the PSD response over the response frequency range. After writing the predictions of RMS vehicle response to an output file, the predictor advances through the track data file by a user-selectable number of points and evaluates new PSDs of track surface and cross-level excitation to apply through the transfer functions.

As in the prior study [TranSys Research, 1997], we have implemented a zero-padding technique in which only a portion of the full FFT window is loaded with data and the balance is padded with zero values. This allows the predictor program to take advantage of the increased number of frequency divisions while retaining sensitivity to localized track conditions. An area of enhancement from the prior study is the addition of a track alignment forcing function. Alignment does explain some of the hit sites and the forces stimulated will lead to further track geometry deterioration. From a track maintenance perspective it provides a useful measure; however, from a derailment risk perspective, alignment-induced roll leads to unloading of the wheel opposite to the flanging wheel and thus does not have the lateral force necessary to produce wheel climb. Therefore, it might be better to ignore the lateral geometry from the perspective of a derailment hazard. The hit prediction would be less successful, but it would focus on those hits that have a higher risk of derailment.

The output of the predictor program and a comparison of its effectiveness with defined regulatory defects are discussed in Chapter 5.

3.2 Non-linear Parametric Model

Much of the Class 3 track is traversed at speeds above the natural roll speeds and below the natural bounce speeds of freight cars. The modified linear model does not predict hit locations as accurately at these intermediate speeds. As will be shown later in Section 4.3, about 15 percent of the hits occurred at these speeds. Even though the predictor identified most of these sites when run at the critical speeds, it would be desirable to know the level of response at the normal track speed.

A non-linear parallel cascade model was trained on data for these locations. A description of the parallel cascade (PC) methodology is provided in Appendix B. The model, which was developed over a relatively short data set of about 1/2 mi. length, was found to predict the location of similar situations quite accurately (see Figure 8). Whereas the linear model locates hit sites within a 50 ft. window, the parametric model identifies suspension dynamics on a step-by-step basis at 1 ft. intervals.

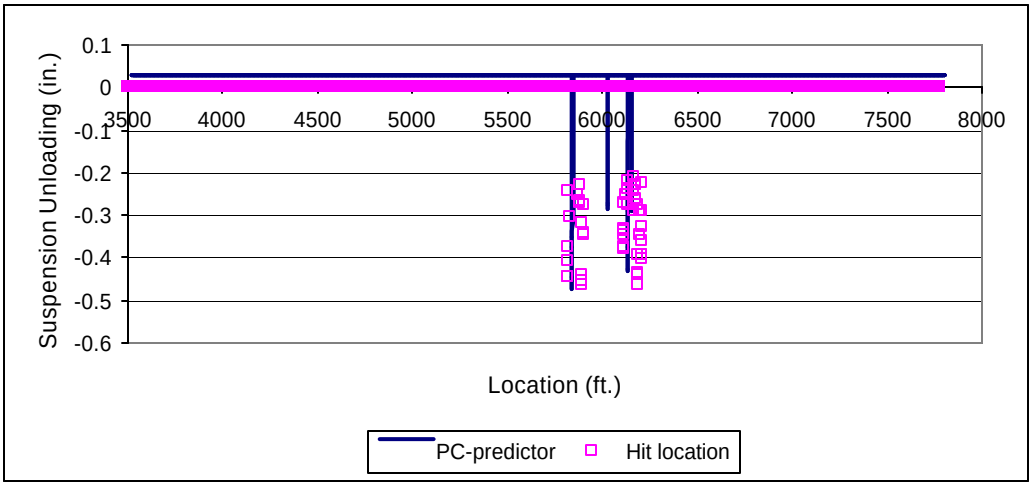

Figure 8 Illustration of parallel-cascade prediction accuracy

The accuracy range of this type of parametric model is tied to the data that it is "trained" with. Although the model was quite successful in predicting hit sites with similar characteristics to the data it was trained on, it had a large number of false positives when applied to a wider range of track conditions. The model would require a significant amount of data to be used as a general-purpose predictor; therefore, it was not pursued further in the present study. However, there is promise in a complementary approach—the PC model could be focused such that it is only trained and applied for specific situations that best complement the quasi-linear model to refine the accuracy and reliability of predicted hit sites.

4 OBSERVATIONS FROM THE DATA / PREDICTOR MODEL

In the course of the test period, each test car traversed each of CN's and CPR's rail systems at least once. Geometry and response data were recorded for all regions of the country and involved subdivisions ranging in quality from Class 1 to Class 5.[4]

In this chapter we present the primary influences observed in the collection of "hit" sites. Each of the following is discussed in sequence:

- Curvature influence
- Vehicle influence
- Speed influence
- Track classification influence
- Relationship to regulatory defects

4.1 Curvature Influence

The data indicate that track curvature seems to further dampen the dynamic response of both empty cars. This is illustrated in Figure 9 and Figure 10, where the quietened response of the car in curves is visually evident. The lower plot in each of the figures is the track profile; the upper plot is the suspension dynamics. In Figure 9 the superelevation is varying in both the tangent and curved sections, but only the tangent section leads to significant stimulation. The second pair of plots (Figure 10) demonstrates a similar quietening in the curve.

It should be noted, however, that the spiral's impact is understated because the trailing right transducer was not functioning at this time. The high load swing evident in the spiral occurs at the trailing left suspension, and the trailing right would have seen a similar unloading. Nonetheless, the dynamic response in the latter portion of the curve is about half the magnitude in the tangent section.

[4] Track classes are a regulatory term used to describe the tighter tolerances required for track geometry at increasing speeds. The maximum freight train speeds allowed on Class 1 through Class 5 tracks are 10 mph, 25 mph, 40 mph, 60 mph and 80 mph, respectively.

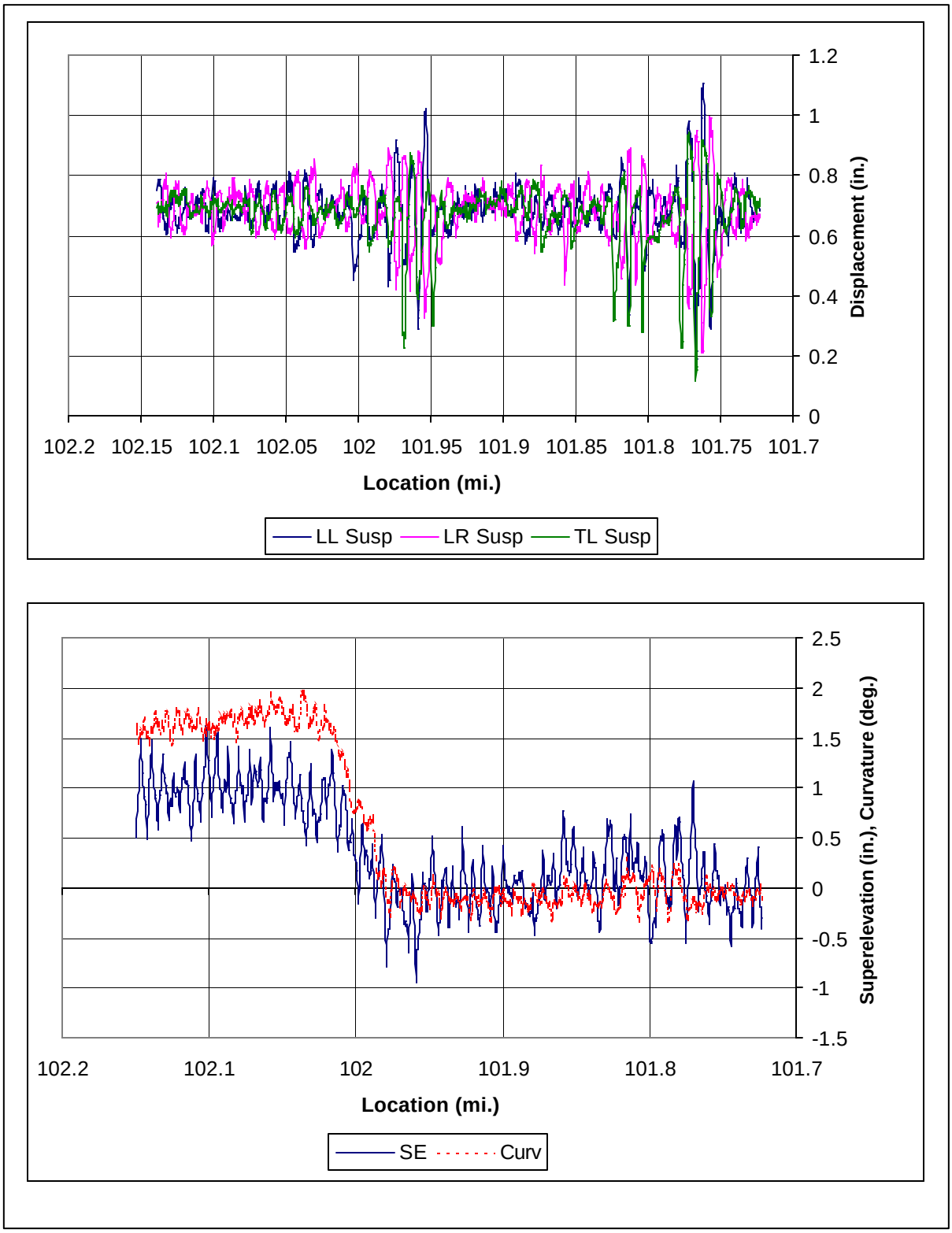

Figure 9 First illustration of curve dampened response

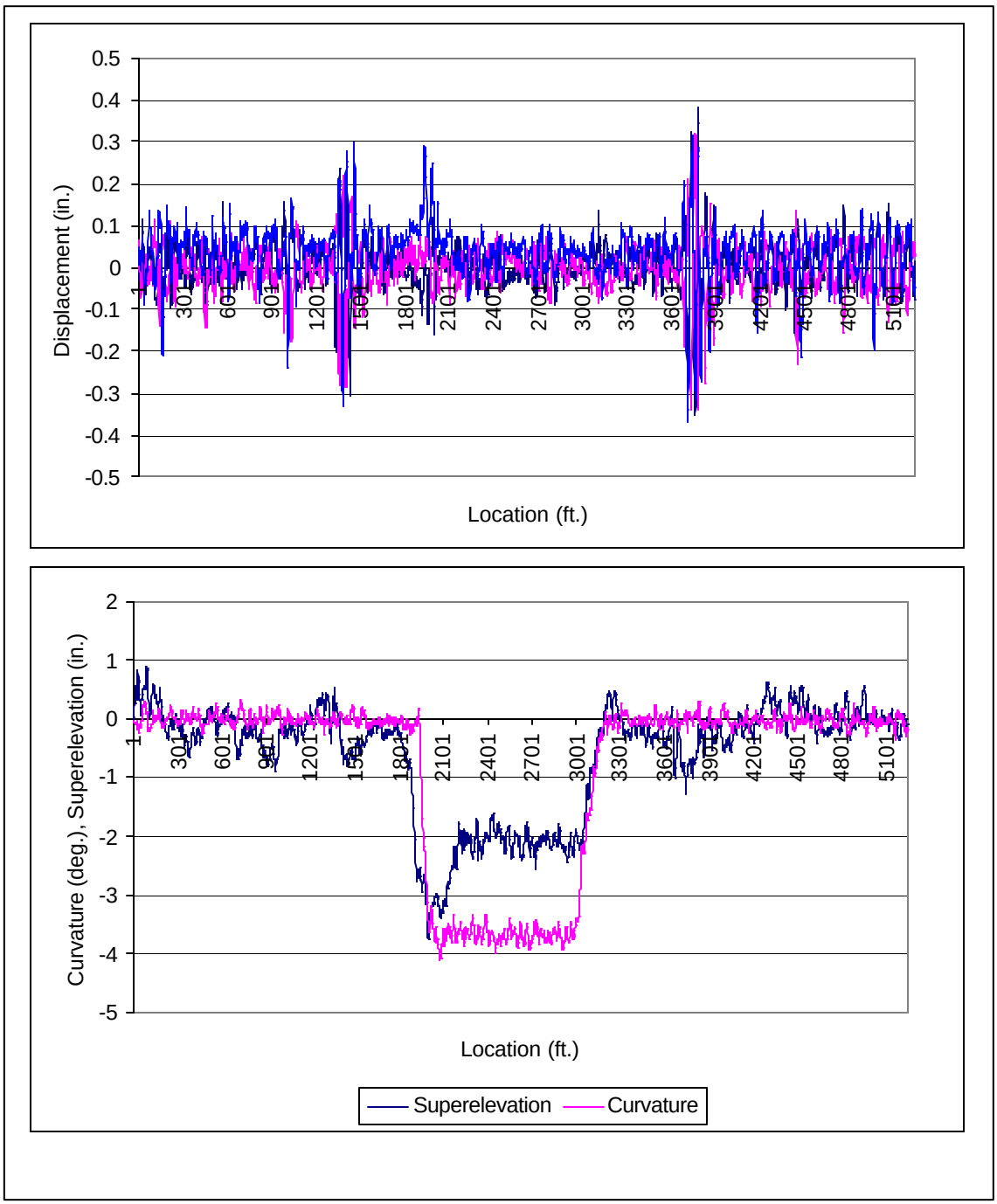

Figure 10 Second illustration of curve dampened response

In comparison with tangent track, the predictor must have an elevated threshold (or a more highly damped characteristic) to predict hits in curves. Figure 11 illustrates this point in a curve with high stimulating cross-level variation with a period almost exactly equal to the car's truck centre spacing. A significant hit is predicted, yet the unloading that occurred is less than 25 percent of static deflection. The test car at this location was the tank car travelling at 39 mph (63 km/h).

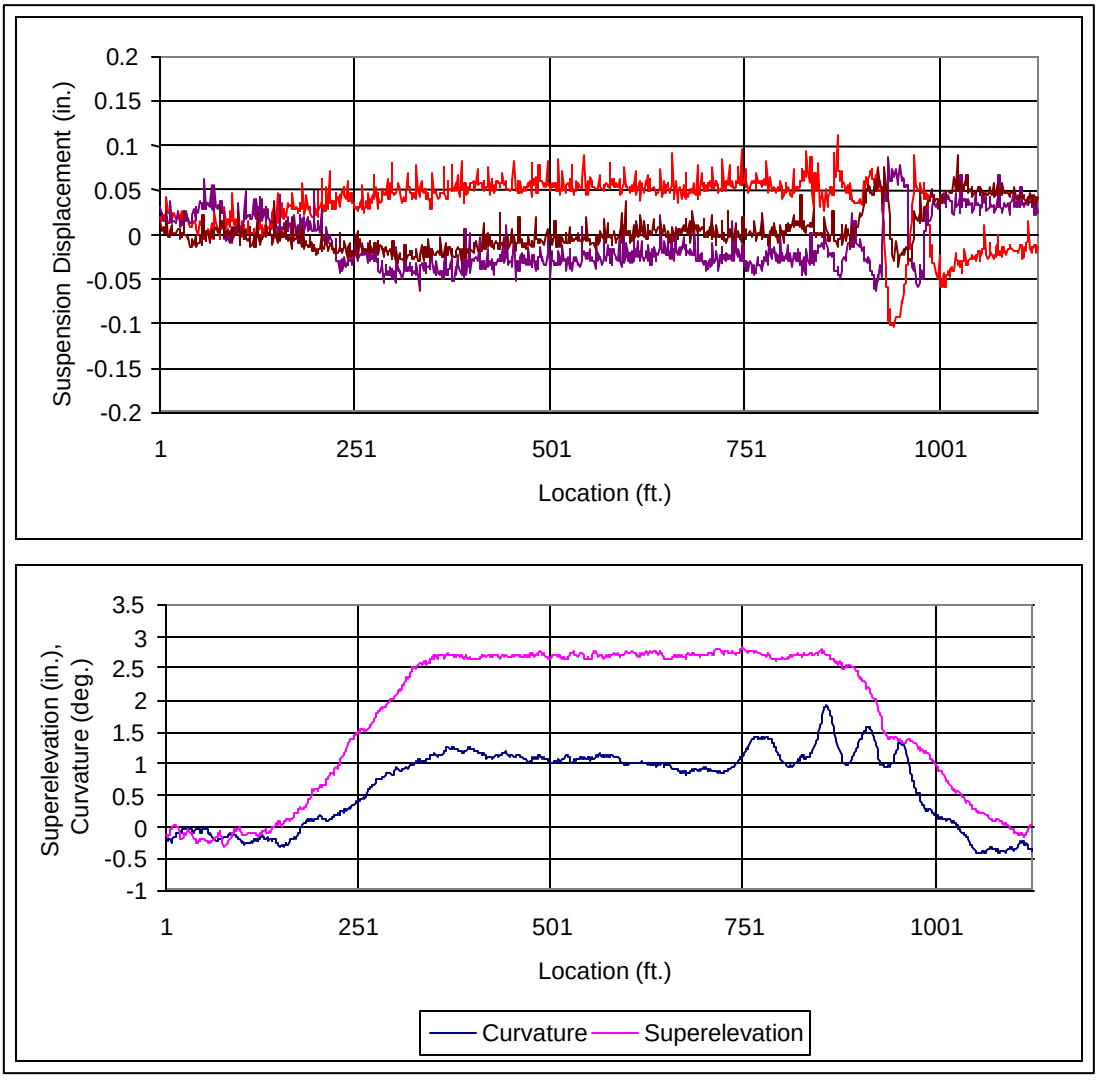

Figure 11 Illustration of a curve with a high prediction error

A possible explanation of the lower response in curves is that the lozenging motion (or parallelograming) of the truck produces a tighter fit and a higher friction force between the wedges and the side frame's wear plates. The resulting higher friction would lead to more damping and fewer occurrences of vertical unloading in curves. However, this apparent advantage in curves requires a few qualifying considerations:

- It is not clear that all cars would respond the same way; the increased friction force might not be as significant for a loaded car.
- It is only in curves that significant, sustained lateral forces are developed, and a lower level of unloading might lead to wheel climb L/V threshold.
- It is possible that in severe situations with unloaded cars, the higher friction force might cause the suspension to lock up and thus the increased friction would present a worse situation that our data would not detect.[5]

Thus, while the data indicate that a given track condition will have a lower probability of exceeding a set threshold in curves than in tangent track, the risks of wheel climb and the uncertainties of suspension lock-up might call for a lower threshold in curves than in tangent track. For this reason, the predictor ignores the dampening effect and, as discussed previously, assesses a reduced threshold in recognition of the higher probability of derailing in curves than in tangent track. It might be possible to relax these assumptions with more detailed testing with instrumented wheel sets.

We note that, while the level of vertical dynamic response at the suspension was mitigated in curves, many hits did occur in curves. Many were on the low rail side and would not lead to L/V forces. However, there were also some occurrences of unloading on the high rail side where derailment concerns arise. The frequency of occurrence and the average level of unloading on the high rail side in curves are illustrated in Figure 12. As can be seen, the worst case was a 77 percent unloading in a 7.1 deg. curve. Obviously, none of the occurrences produced a derailment, further highlighting the issue of what should be considered a derailment hazard. One would need to have insight into the wheel rail forces at these hit sites to better assess this question.

4.2 Vehicle Influence

The relative hit frequency of the two cars is compared for three different subdivisions in Table 3. The weighted-average hit ratio shown in the bottom row of the table has a weight of 2 for 80 percent unloading and 3 for 90 percent unloading. The results shown are representative of the full test set. In general, the hopper car experienced a higher frequency of hits than the tank car, although the results are somewhat exaggerated by the poorer performance of the hopper car on jointed rail branch lines such as Subdivision B in Table 3.

---

[5] We note that the suspension displacement measurement does not give a direct indication of what is happening at the wheel. If the suspension and axles did lock up, there would be a minimum variation in bolster activity recorded and no indication if a wheel lifted off the rail.

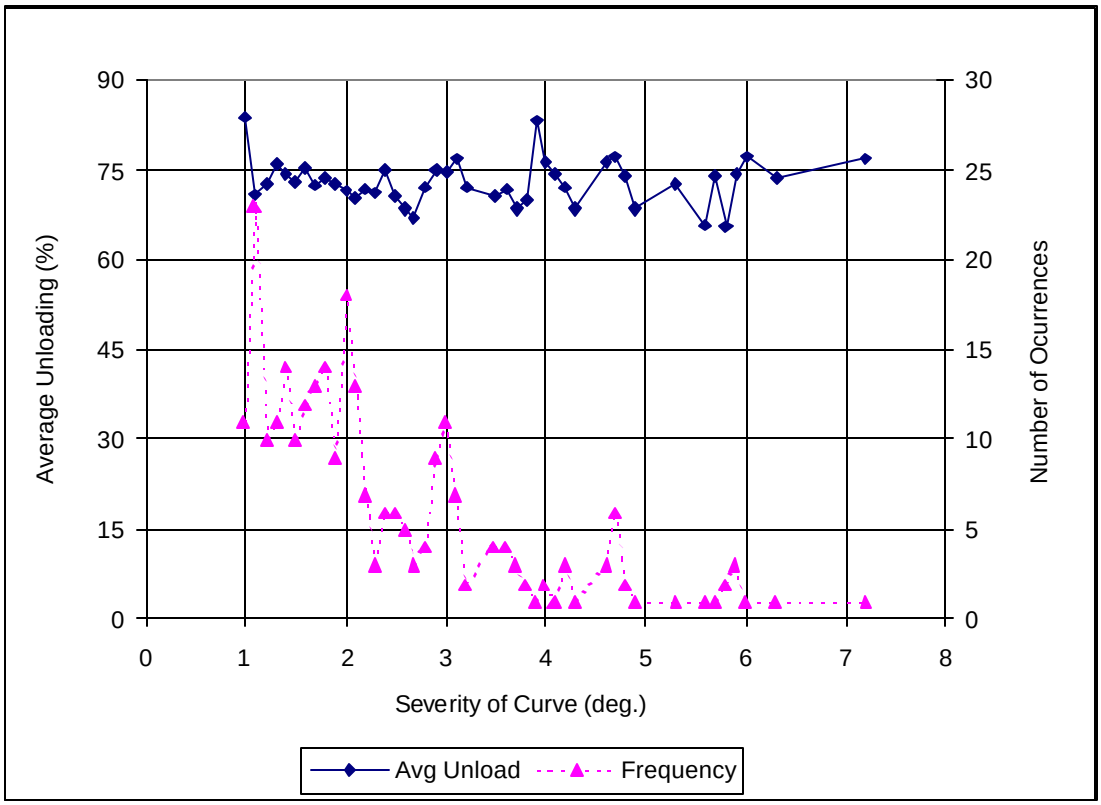

Figure 12 Frequency of unloading on the high rail side in curves

The hopper/tank hit ratio is almost ten times higher for the Class 2 jointed rail subdivision (Subdivision B) than for the Class 4 continuous welded rail subdivision (Subdivision C), which was mostly traversed at a 60 mph test speed.

Table 3 Comparison of tank car and hopper car hit frequency

%-unload	Subdivision A (Prairie main)		Subdivision B (Prairie secondary)		Subdivision C (N. Ontario)	
	Hopper	Tank	Hopper	Tank	Hopper	Tank
66	75	11	643	30	28	12
80	17	1	199	7	6	0
90	4	0	37	2	2	0
Weighted average H/T hit ratio[#]	9.3 to 1		23.0 to 1		3.8 to 1	

[#] Weighting is H(66%) + 2 * H(80%) + 3 * H(90%)

We note that the two test cars travelled across the three subdivisions shown in the table at different times of the year and at somewhat different train speeds. Both of these factors could influence the number of hits. Nonetheless, the data highlight a situation that is also supported by the predictor software—the hopper car is (with a few exceptions) more readily unloaded. We also note that the hopper car (with a lower static weight and

slightly stiffer suspension than the tank car) required a spring travel of 7.25 mm (0.29 in.) to register a hit, while the tank car required a spring travel of 11.38 mm (0.45 in.) to register a hit.

4.3 Speed Influence

As noted, the comparison of tank car hits and hopper car hits discussed above might exaggerate the relative performance of the two cars. In particular, the significant differential between the two cars in Subdivision B of Table 3 is significantly influenced by the speed limits in this subdivision. The speed was mostly in the range of 20 to 25 mph, which corresponds with the speed at which the natural roll frequency of the hopper car is stimulated by single events and by the repetitive input of rail joints (23 mph for 39 ft. rails). On the other hand, the tank car has a truck spacing and natural frequency that leads to a critical input at 30 mph. This factor is illustrated in Figure 13, which shows the predicted results for a mixed Class 2 and 3 subdivision if it were traversed at specific speeds.

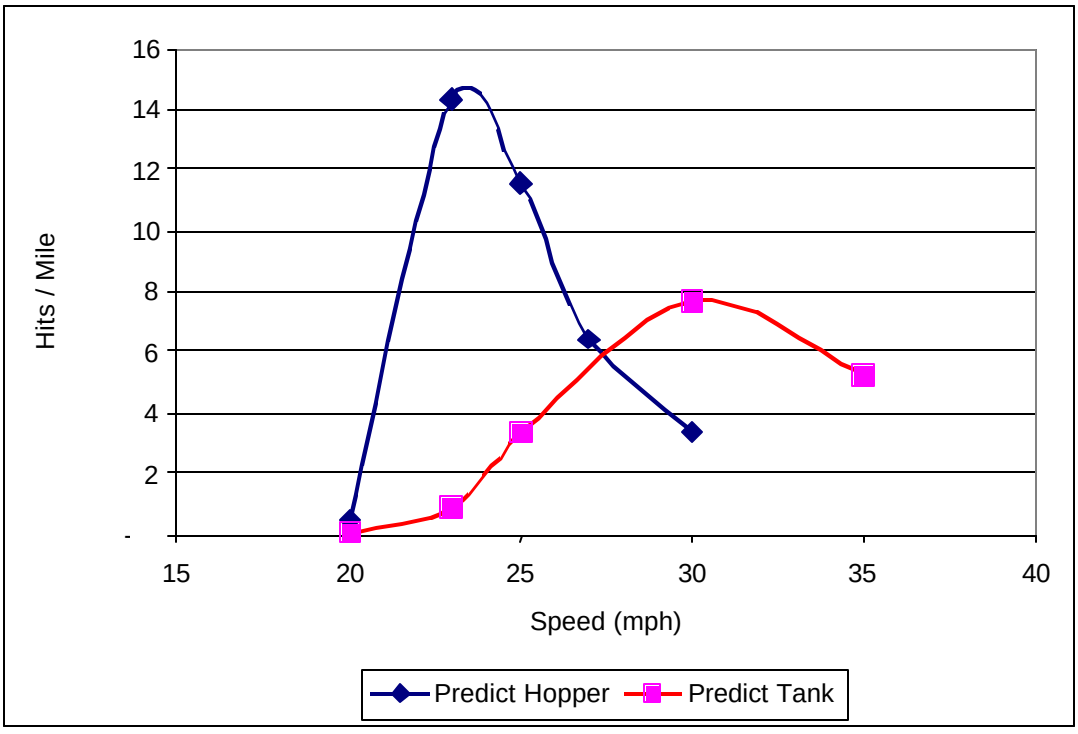

Figure 13 Predicted hit frequency versus train speed (Class 2 track, jointed rail)

As can be seen, the tank car peaks at 30 mph and the hopper car at 23 mph. It should be noted that the hit count for the tank car at its peak of 30 mph is double the hit count of the

hopper, while the hit count of the hopper car at its peak of 23 mph is 14 times that of the tank car.

Also of interest is the fact that the response of both cars was significantly quieted at speeds of 20 mph and lower. Figure 14 and Figure 15 illustrate the influence of a speed reduction to 10 mph on the hopper car and tank car, respectively. The effect of 20 mph on the hopper car can be seen to be equally effective in Figure 18.

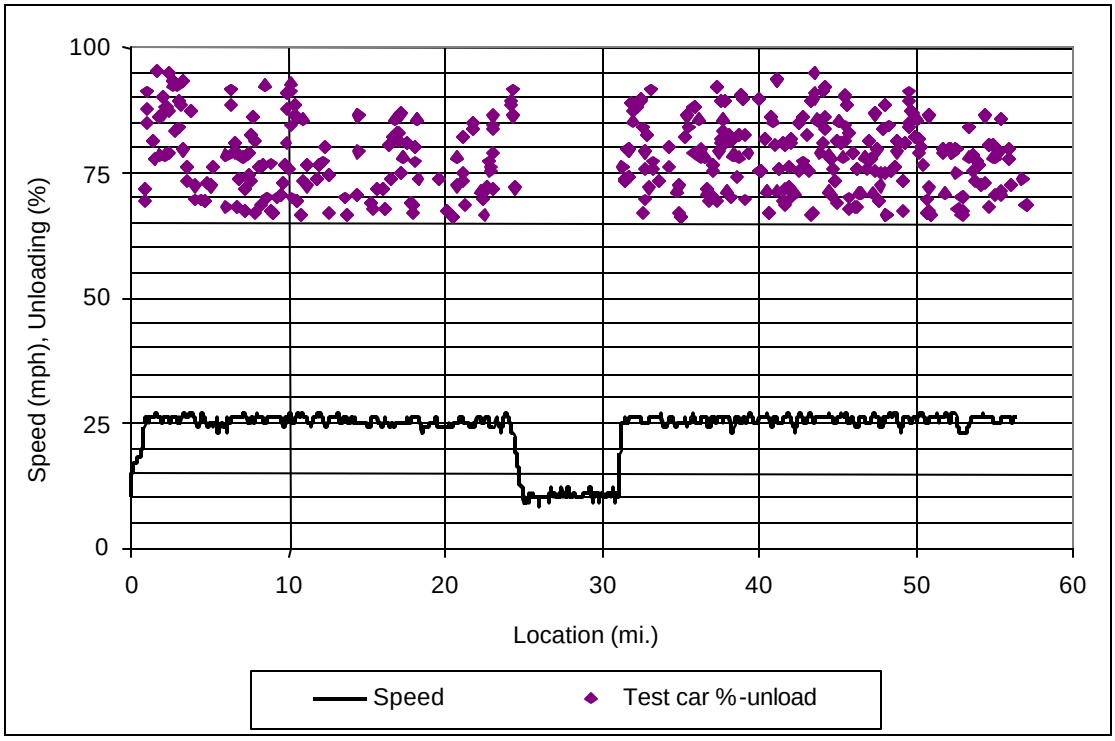

Figure 14 Effect of 10 mph speed limit on the hopper car

We caution that the two test cars were empty—a loaded car would be stimulated at lower train speeds. Nonetheless, the results raise the question of what the most effective speed limits would be for locations that are identified as a derailment risk. For the empty hopper car, a speed limit of 25 mph could elevate the derailment risk, while a reduction from 25 mph to 20 mph could be just as effective as a reduction to 15 or 10 mph.

Another consequence of the critical roll speeds that are discussed later in subsection 4.4.2 is that hits that occur in the 35 to 50 mph range are usually predicted to be much higher at the critical roll speed than at the test train speed. This means that hit sites can be located by using a few critical speeds rather than having to test the response with a large number of train speeds.

The influence of the critical roll speed range is also illustrated in the overall hit frequency versus train speed for the test period (see Figure 16). However, the results are strongly influenced by the track conditions at the test speed, as is discussed in Section 4.4.

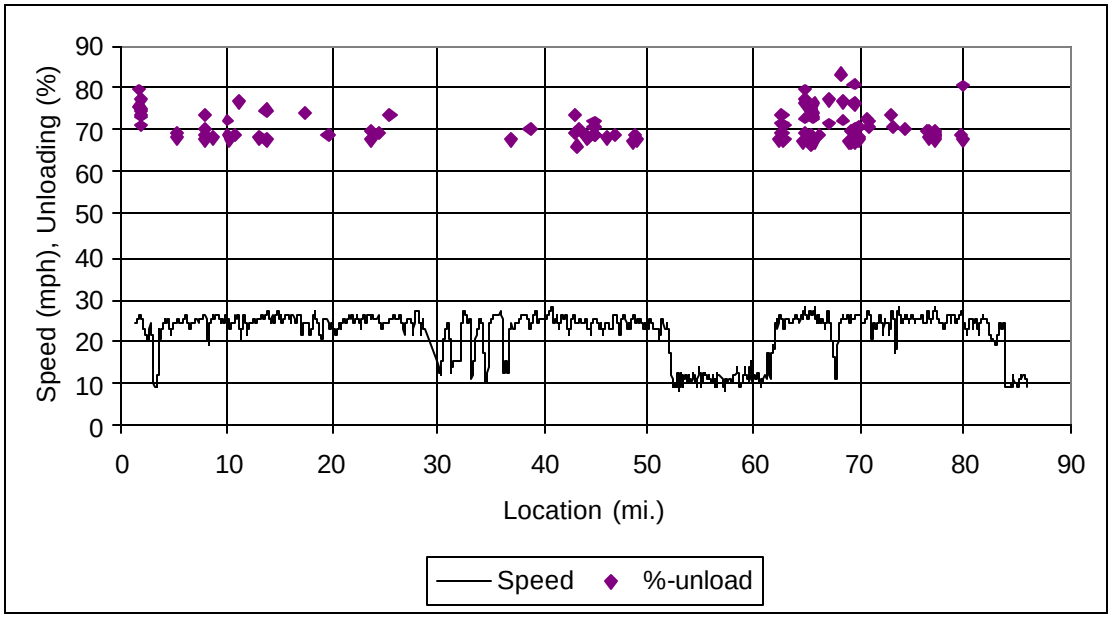

Figure 15 Effect of 10 mph speed limit on the tank car

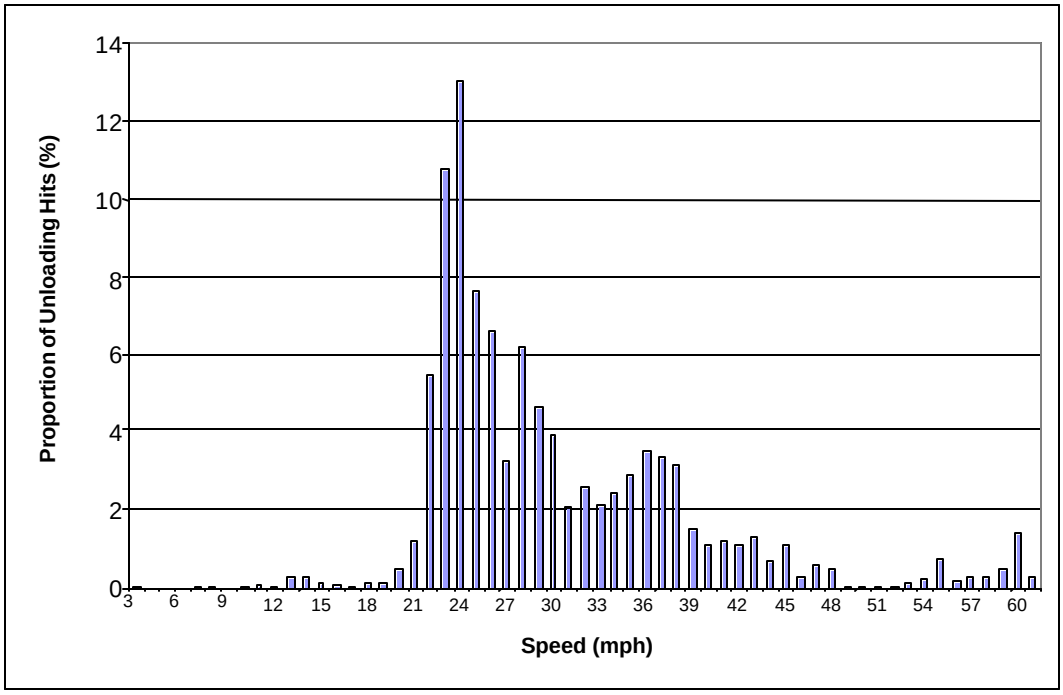

Figure 16 Distribution of unloading incidents versus train speed

4.4 Track Class Influence

It should be noted that the speed influence noted in Section 4.3 is not simply a car response phenomenon. The bulk of the lower speed hits were generated on Class 2 track on a small number of secondary lines. The high hit frequency on Class 2 track is a combination of the higher cross-level variation on jointed track and the fact that the imposed speed limit is close to the peak roll response of the empty cars.

Table 3, which was previously used to illustrate the higher proportion of hopper car hits, also illustrates the impact of track classification. The Class 2 track generated about 20 times more hits that the Class 4 track, and the mixed Class 3 and 4 track generated about three times as many hits. However, as discussed in Section 4.3, the hit ratio also reflects the speeds at which the test trains were operated. The Class 4 track was traversed at close to 60 mph, a speed that does not generate significant roll response.

In the following subsections we present the unloading locations and the relative accuracy of the predictor for a range of subdivisions.

4.4.1 Example of High-Speed Response

Figure 17 illustrates the location of actual hits and the vehicle response predicted for the hopper car over Class 4 track. The hits are identified with square symbols while vertical dashed lines identify the predictor output. The plot also includes the speed at which the test train was operated. As can be seen, the test train operated within a speed range of 45 to 60 mph and most of the hits occurred near 60 mph.

While there were 45 individual hits (suspension unloading beyond 66 percent), many of the hits are actually multiple occurrences of suspension unloading at the same site. Table 4 compares the number of unloading hits with the number of sites involved. The count of 45 hits represents 16 separate sites, three of which are over 100 ft. in length and encompass 32 of the hits. It should be noted that the three responses exceeding 90 percent were severe enough to result in a suspension lift-off, as indicated by the 16 boxes above 100 at three locations.

Table 4 Number of hits versus unloading threshold, Class 4 track

Threshold	Hit Count	Hit Sites
67%	45	16
80%	34	7
90%	24	3

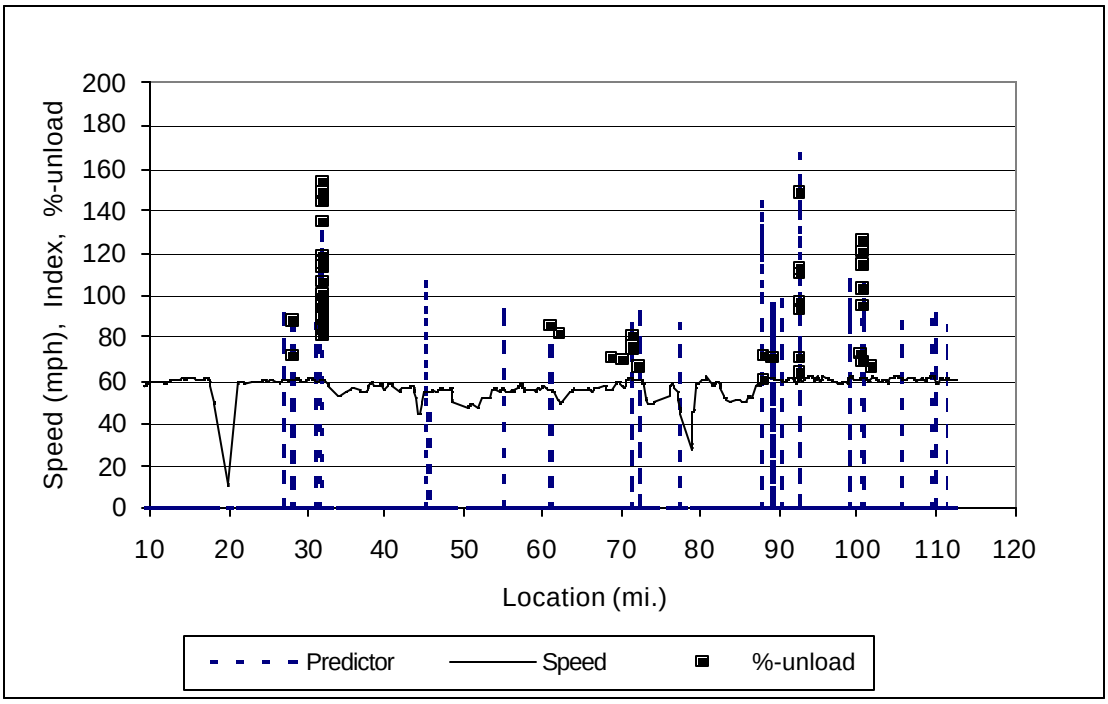

Figure 17 Hopper car hits, Class 4 track

The predictor identifies the three worst hit sites, all but one of the seven hit locations exceeding 80 percent unloading, and all but three of the lower level hits. There were 11 sites predicted to have hits that did not. There is, of course, a trade-off in the number of missed hits and the number of false predictions. The threshold of the predictor algorithm can be lowered to recognize all hits, but will elevate the number of false positives in the process. Our selection of a threshold weighed the prediction of 80 percent-unloading-hits more heavily. The elevation of false positives was not considered as a significant factor since the false positive predictions reflect track that produced a significant dynamic response except for one that remained below the threshold. We assess the predictive performance against that of the existing regulatory defects in Section 5.1.

4.4.2 Example of Low- and Medium-Speed Response

Figure 18 illustrates the hopper car unloading sites predicted over a 133 mi. subdivision, 89 mi. of which are Class 3 and 44 miles of which are Class 2. The actual hits are shown with $*$ symbols, while the predicted hit locations are shown with vertical lines. The speed of the test train is also shown on the plot and highlights the influence of train speed/track class. In comparison with the Class 4 track discussed in subsection 4.4.1, there are significantly more hits generated on this subdivision.

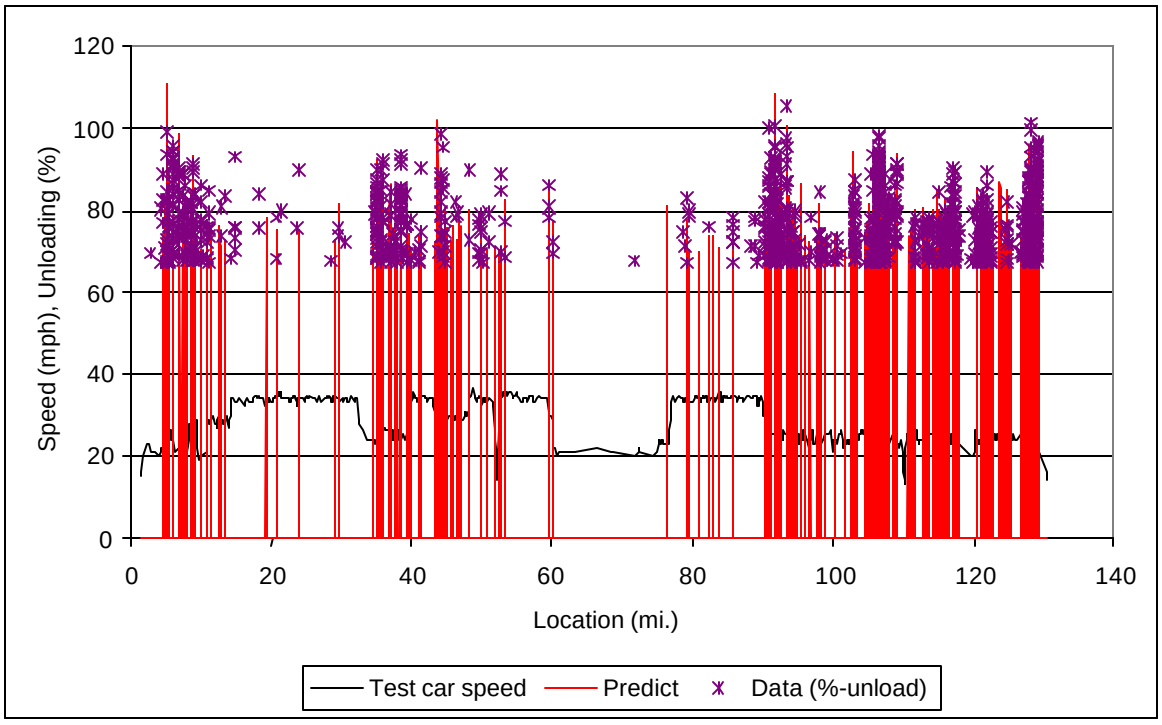

Figure 18 Hopper car hits, mixed Class 2 and 3 track

One can see that the hit density is much higher on the 25 mph (Class 2) sections than on the 30 and 35 mph (Class 3) sections. The effectiveness of the 20 mph speed limit between mile 61 and 78 is also evident.

It is difficult to quantify the predictor's effectiveness in locations with this density of hits. The predicted sites are seen to follow the hit density quite well. In effect, the density of hits at some locations leads to some relatively long continuous-hit segments. As summarized in Table 5, there were 1,086 hits in this subdivision. However, of the 1,086 "hits" associated with ">67 percent unloading", many represent multiple hits at the same location or continuous rolling for long segments.

Table 5 Number of hits versus unloading threshold, Class 2 and 3 track

Suspension Unloading Threshold	Hit Count
67%	1,086
80%	327
90%	77

Thus, the count of 1,086 hits in the above table represents:

375 locations, of which:

215 are local hits, and

160 involve continuous roll track segments with:

an average length 200 ft., and

a maximum length of 1,300 ft.

As compared in more detail in Section 5.1, the TC defect/exception report, which is generated by the geometry car's software, indicates 17 urgent and 330 priority sites with surface (non-gauge) occurrences for this track.

5 RELEVANCE TO REGULATORY DEFECTS/EXCEPTIONS

Railways refer to departures from the regulatory standard as either a "defect" or an "exception". We will use the term "defect" for ease of reporting in the following discussion.

5.1 Comparison of Predictive Accuracy

In this section we provide a comparison of hit sites with regulatory exceptions/defect locations for a range of subdivisions and the relative accuracy of the predictor software and regulatory definitions in locating track conditions that produced hits. In the subsequent subsections we discuss the relevance of some specific defect categories.

The most significant geometry stimulus of suspension unloading at most train speeds is cross-level variation, with surface and alignment geometry exerting increasing influence at speeds over 35 mph. In comparing the locations of regulatory defects with hits, we have assessed only these types of defects (i.e. gauge defects are not considered relevant in this comparison).

The index chosen for the accuracy comparison was:

$$AI = P - 3 \times M90 - 2 \times M80 - M67 - FP$$

where:

AI is the accuracy index

P total number of hit sites accurately predicted

M90 is the number of missed hits that exceeded 90 percent unloading

M80 is the number of missed hits that exceeded 80 percent unloading

M67 is the number of missed hits that exceeded 67 percent unloading

FP is the number of false positives

In general there was a very poor relationship between hit sites and regulatory exceptions/defects. However, we note that the hits are associated with the specific speed of the train that pulled the test car. As noted previously, the cars have certain speeds at which they are most readily stimulated. The test speed is close to the worst-case speed on Class 2 tracks, but not on the other track classes. Thus, the low hit count on the higher track classes is influenced to a certain extent by the test speed. For this reason, we ran the predictor software over the same tracks but at the critical speeds to "predict" what the hit locations would have been under those conditions. This combination of actual and

predicted hits provides a more complete assessment of the relevance of regulatory defects to stimulated dynamic car response. This is illustrated in the following discussion of four different subdivisions.

5.1.1 Class 4 Prairie Subdivision - Hopper Car

The locations of defects, unloading hits and predicted hits at critical speeds are illustrated in Figure 19 for the same Class 4 subdivision that was discussed in subsection 4.4.1

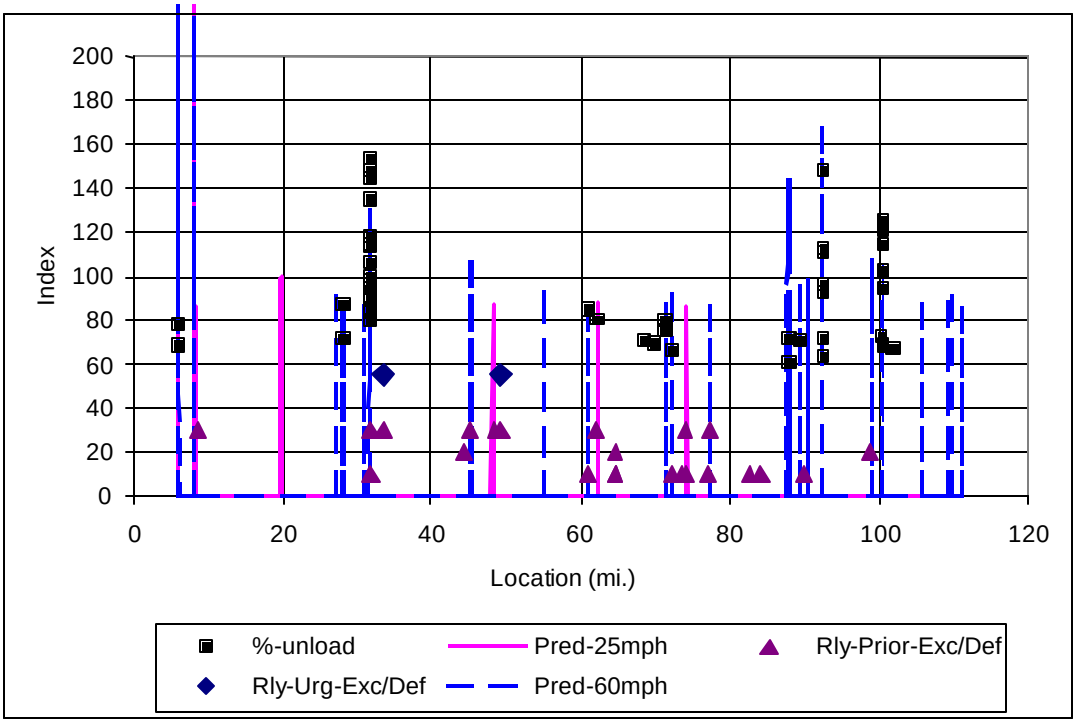

Figure 19 Predicted, actual and regulatory defects, Class 4 track

The test hopper car exhibited 45 hits representing 16 locations in traversing this subdivision. This particular subdivision was traversed at relatively high speed, which could understate the number of potential roll-response hits. Running the predictor program for the same subdivision at a roll-stimulating speed of 25 mph led to additional hit sites. The roll speed added four new sites to the predicted hit list, one of which coincided with a hit that had not been predicted at the train speed. The other three were close to the regulatory defect sites.

The geometry car found 2 urgent and 22 priority defects/exceptions in the same trip across this subdivision. Neither of the two urgent defects was near a hit site, nor did they register with the predictor at either speed. Four of the priority defects were close (although none was closer than 500 ft.) to hit sites, and six of the priority defects did not align with hit sites but were close to predicted hit sites (either for non-test speed or with

false positive sites). Two of the three worst hit sites and eight of the other hit sites were not identified as either priority or urgent regulatory defects.

Ignoring the three sites where the roll predictor coincided with regulatory defects, the two indices are summarized in Table 6.

Table 6 Predictor/regulation comparison, Class 4 track

Component	No. Hit Sites	Regulation	Predictor
Predicted Hits	16	4	13
(>90%)	3	1	3
(80% to 90%)	4	1	4
(67% to 80%)	9	2	6
False Positives		20	13
Weighted Index		**-39**	**-3**

The predictor software is significantly better than the regulatory definitions in isolating locations that generate hits. The two urgent defects were both false positives and the 23 priority defects identified four of the hit sites.

5.1.2 Class 3 Mountain Subdivision - Hopper Car

Figure 20 illustrates the predicted hits, actual hits and regulatory defects for a Class 3 mountain subdivision. The regulatory defects are shown on the plot at a magnitude of 55 for urgent defects and 40 for priority defects. The number of defects and their coincidence with predicted and/or hit sites were much better for this subdivision. Still, the predictor outperformed the regulations as summarized in Table 7.

It should be noted that 90 percent of the hits occurred in curves or spirals in this subdivision. While this might be intuitively obvious for mountain terrain, it is noted to counter any impression that might have been made in the previous discussion of the dampening effects of curvature on vertical dynamic response. Even though the response was dampened, the high incidence of curves and spirals lead to a predominance of hits in these locations.

Table 7 Predictor/regulation comparison, Class 3 mountain subdivision

Component	No. Hit Sites	Regulation	Predictor
Predicted Hits	33	8	22
(>90%)	4	0	4
(80% to 90%)	10	4	7
(67% to 80%)	19	4	9
False Positives		27	26
Weighted Index		**-58**	**-20**

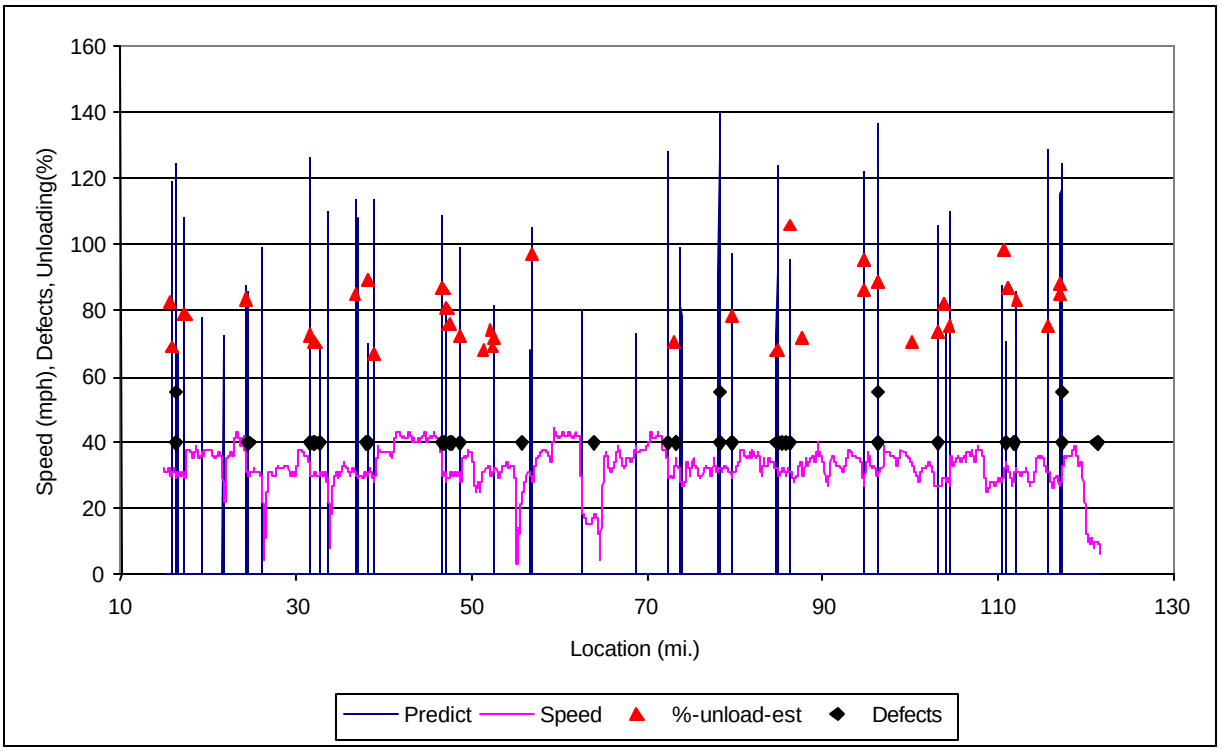

Figure 20 Predicted, actual and regulatory defects, Class 3 mountain subdivision

5.1.3 Class 3 and 4 Mountain Subdivision - Tank Car

The test tank car experienced only one hit on this mixed Class 3 and 4 mountain region subdivision. With such a small incidence of actual recorded hits, it is difficult to make a quantitative assessment of the accuracy of the predictor. The predictor was run for both the hopper car and tank car both at their peak response speeds (25 mph and 30 mph, respectively) and at the speed limit.

Figure 21 compares the regulatory defect locations with the single tank car hit site (mile 148.5) and predicted hit sites. For illustrative purposes, the predicted hit sites are shown at the speed at which the hit is predicted to occur rather than at the magnitude of the predicted hit. In comparison, there were 13 urgent and 315 priority defects defined by the regulations. The urgent defects are shown on the plot at an index value of 45 and the three levels of priority are shown at 30, 20 and 10, in order of decreasing priority. The hit site was denoted by a level-3 multiple priority defect, which is discussed in more detail in subsection 5.2.2.

The predictor assessed 43 hits involving 14 hit sites by either the tank car or the hopper car at speeds near the test train speed and the actual hit site was one of the predicted sites.

The model predicted another 30 hit sites that are not shown on the plot. These occurred at locations assumed to have 35 or 40 mph speed limits but where the test train had slowed to 20 mph or less. The hits might reflect locations that had temporary speed limits for geometry problems.

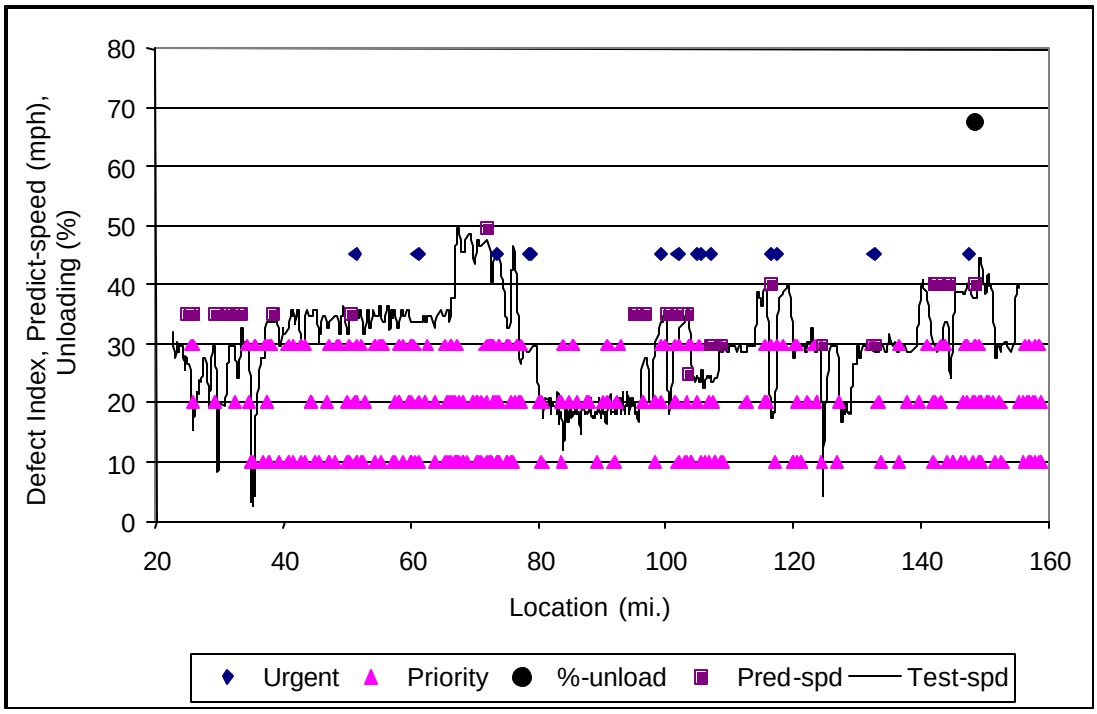

Figure 21 Predicted, actual and regulatory defects, Class 3 and 4 mountain subdivision

5.1.4 Class 4 Canadian Shield Subdivision - Hopper Car

Figure 22 compares hopper car hits, model predictions and regulatory defects for a 300 mi. long Northern Ontario subdivision. There were 83 hits involving 43 separate sites. Urgent regulatory defects are shown at an index of 55 and the three levels of priority are shown at 30, 20 and 10, in order of decreasing priority. The model prediction index is shown as vertical lines (solid lines indicate predictions at the test speed and dashed lines indicate predictions at 25 mph). Table 8 summarizes the number of hit sites and the relative prediction accuracy.

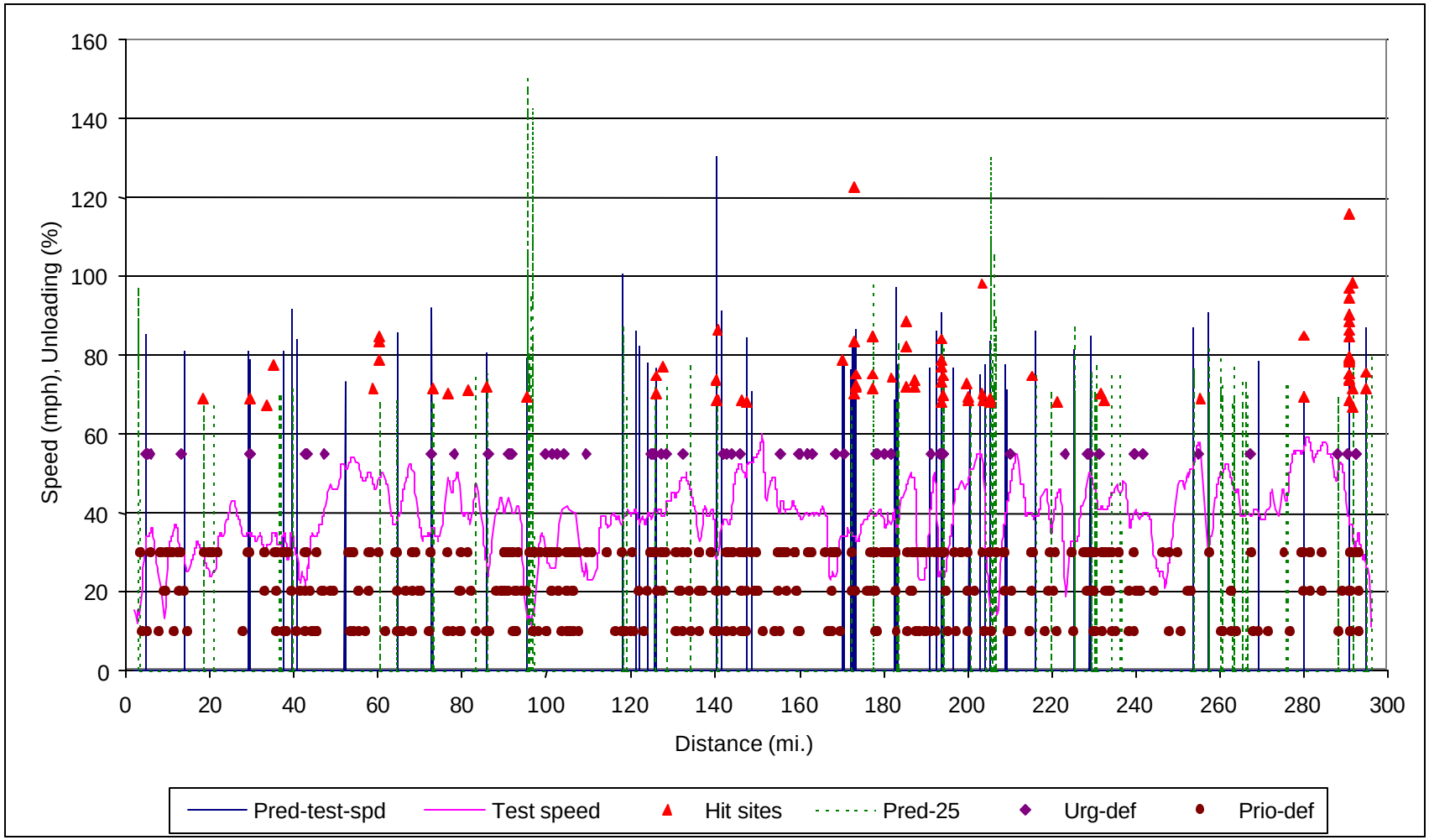

Figure 22 Predicted, actual and regulatory defects, Class 4 N. Ontario subdivision

Table 8 Predictor/regulation effectiveness, Class 4 N. Ontario

Component	# Hit Sites	Predictor	Urgent	Priority + Urgent
(>90%)	4	4	1	4
(80% to 90%)	6	5	1	4
(67% to 80%)	33	13	6	31
False positive		47	54	436
Weighted Index		**-12**	**-20**	**-411**

The predictor can be seen to outperform the urgent defects in both the number of hits predicted and the number of false positives generated. When the priority defects are included, the predictor has a significant overall performance advantage. The priority defects identify more than twice as many lower-level hits, but at the cost of almost 10 times as many false positives.

5.1.5 Mixed Class 2 and 3 Subdivision - Hopper Car

Table 9 compares the hit density with the regulatory defect density for the mixed Class 2 and 3 subdivision shown in Figure 18. One can see that, although the frequency of unloading was much greater in the Class 2 track segments, the frequency of defects is much greater in the Class 3 track segments. While the ratio of Class 2 to Class 3 hits is about 4.5 to 1, the ratio for priority defects is just the inverse (i.e. 1 to 4.5). The ratio for urgent defects is 1 to 1.5.

While the mainline subdivisions exhibited many more regulatory defects than hit sites, the Class 2 line segment exhibits just the opposite—many more hits than defects. The frequency of regulatory defects on Class 2 track is influenced by the more relaxed tolerances that are allowed at the lower speed limit.

Table 9 Comparison of hit and defect frequency, Class 2 and 3 track

Track Class	Length (miles)	Occurrence frequency (/mile)		
		Recorded hits	Urgent defects	Priority defects
Class 2	44	18.20	0.11	0.75
Class 3 *	73	3.89	0.15	3.41

* the 20 mph section of Class 3 track seen in Figure 18 is excluded

5.2 Insight into Specific Regulatory Defects

5.2.1 Unbalanced Superelevation Influence

We were asked to assess the influence of superelevation in tangent track on suspension unloading. Figure 23 is from a Class 2 track with a stretch of *design-elevation-tangent* exceptions. The hit locations for this track can be seen to be associated with variations in elevation rather than the actual magnitude of the average elevation.

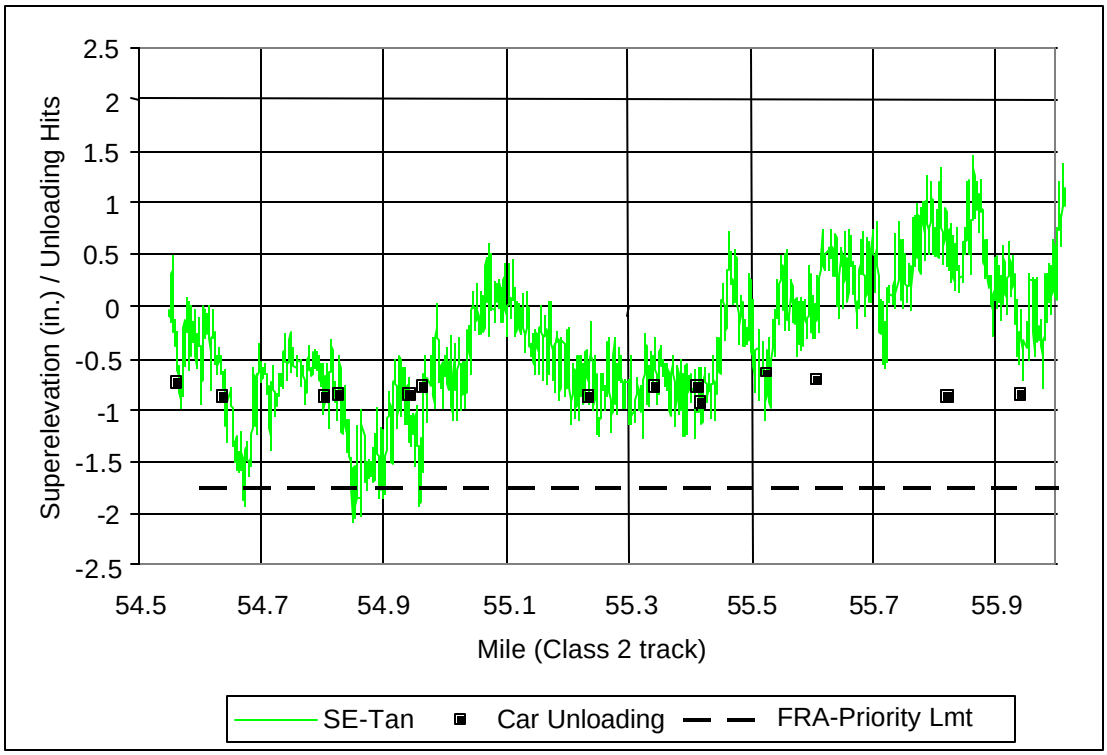

Figure 23 Unbalanced superelevation in tangent track

Perhaps a better illustration of what happens in track with superelevation is the segment of track shown in the two aligned plots in Figure 24. The plots illustrate a shallow—0.5 deg.—curve with 2.5 in. of superelevation taken at 40 mph. The situation is the same as 2 in. of superelevation in tangent track. The carbody weight is seen to shift to the lower rail, but does not in itself produce a hit. The higher unloading occurs at a rapid change of superelevation in the tangent track segment following the curve. Since the superelevation does occur in a curve, it does not represent a regulatory exception. However, if the curve were a 0.1 deg. curve instead of a 0.5 deg. curve, the result would not be much different.

Nonetheless, a steady-state average elevation will make the vehicle more sensitive to local variations. The 20 percent unloading associated with the 2 in. unbalanced

superelevation in Figure 23 and Figure 24 means that changes in elevation need only produce an additional 47 percent unloading to reach the 67 percent unloading limit.

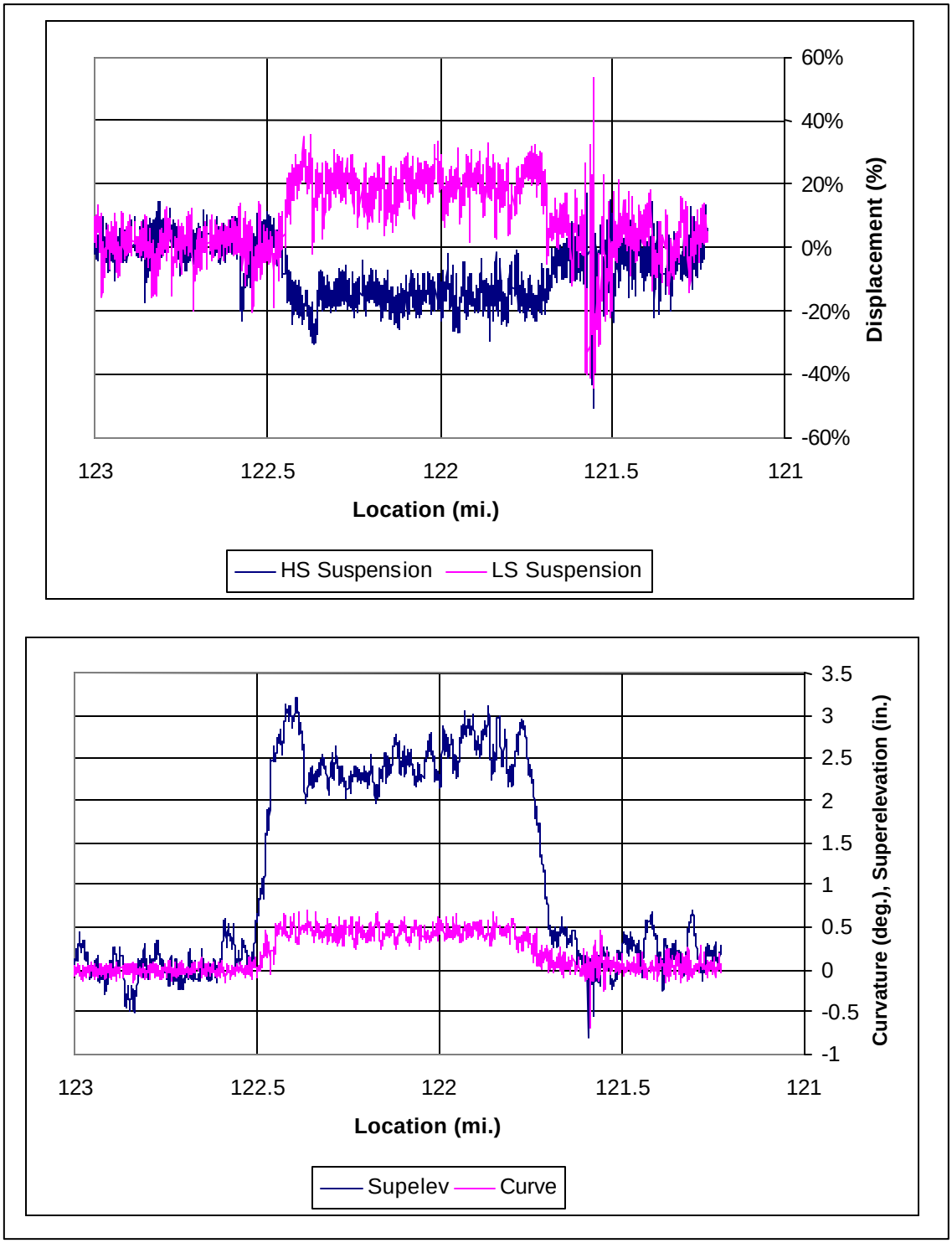

Figure 24 Unbalanced superelevation in very low curvature

5.2.2 Combined Priority Defects

The principal non-gauge defects occurring in the comparisons described in subsection 5.2.1 were rate of change (RC) in superelevation (SE), twist or warp conditions. We did find that these conditions had an influence on the magnitude of a hit, but that the magnitude of twist was not in itself a good predictor. Large values could be traversed without impact, whereas lower values could amplify hits if other stimulating factors were present. Thus, a steep but steady spiral could be negotiated without incident, but a less steep spiral with one or more reversals of slope would be more likely to produce a hit.

The predictor inherently includes the contribution of the different geometry inputs at a given location. In the case of the twist (or RC-SE) defect noted above, it is possible to say that these defects are of much more concern if they occur in combination with other defects that highlight the possibility of an inflection point occurring. Thus, a lower magnitude RC-55, when combined with a priority roll defect or an alignment defect, could be more of a hazard than a high-magnitude RC-55 on its own.

Figure 25 presents the details of the single tank car hit in the mountain subdivision discussed in subsection 5.1.3 (see Figure 21). As previously noted, this subdivision had 13 urgent defects and 315 priority defects. The hit site is seen in Figure 25 to have been stimulated by a superelevation inflection point in the tangent section, just before the spiral. There are three priority defects in the full track segment. The lead-in spiral has an excess rate of change in superelevation over 31 ft. (beginning at location 311). As can be seen in the aligned plots, this defect did not stimulate a car response.

The superelevation inflection point (at location 200) that stimulates the hit exhibits two level-3 priority defects:

1. an offset from a 62 ft. chord (warp), and

2. a rate of change in excess of the limit over 55 ft.

The fact that the RC condition existed for over 100 ft. is an indication that there is more than one roll stimulus to the car. This combination (a warp condition coupled with an RC condition with either one extended beyond a single 62 ft. length) is in fact a much improved simple predictor. Of the 315 defects, there were 25 multiple RC/warp sites, 8 involving level-3 priority and just 4 involving lengths for one or the other measure in excess of 62 ft.

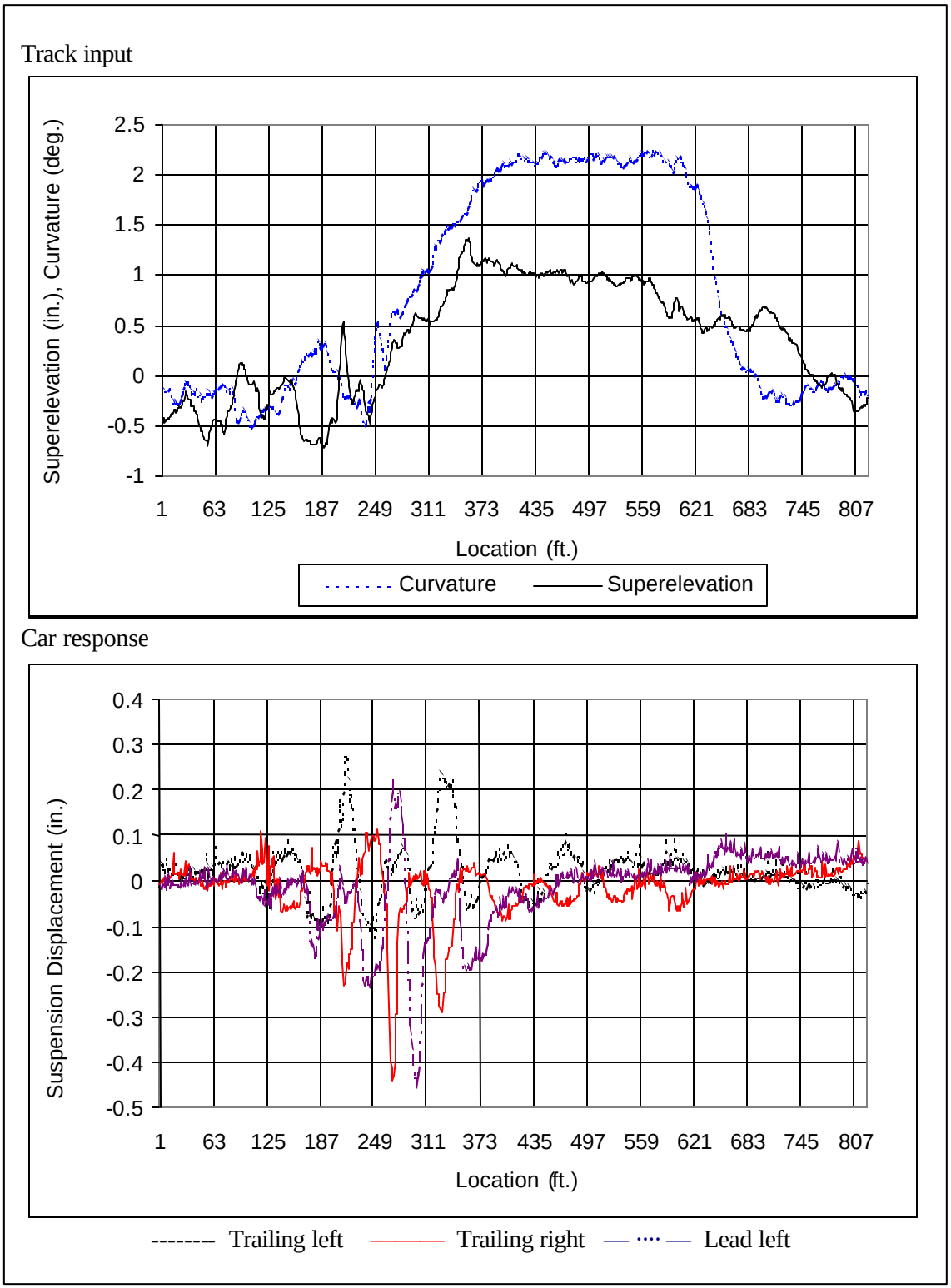

Figure 25 Car dynamics at a multiple priority defect

We note that, while the above combination helps to explain the response at this site, the predictor also recognizes what is happening at the truck spacing and at critical distances determined by the vehicle's critical response frequencies. As was demonstrated in Section 5.1, there are many severe hit locations that do not exhibit any priority defects.

Figure 26 presents the recorded tank car response at a site that only registered a level-2 priority defect. The top plot in the figure presents the recorded displacement data for the tank car suspension. The middle plot shows the track profiles (cross-level, curvature and surface) that generated the hit. The bottom plot shows the simulated response of the track car at the hit site.

The simulated car response is seen to include a low-frequency roll triggered by the cross-level variation and a higher frequency bounce. The combination of both modes on the spiral leads to lift-off at one side of one truck and significant unloading at the other locations.[6] The critical element in triggering the violent bounce response is the smaller variation "ripples" evident in the surface profile rather than the twist introduced by the rapid rise on superelevation.

[6] The fact that this hit occurred in a shallow curve highlights the issue of what should be considered a derailment risk. We note that there were only a few such instances of unloading to this magnitude in 12 months of testing and obviously none produced a derailment. While it would have been nice to have the insight of an instrumented wheel set at this location, it would be extremely expensive to send an instrumented wheel set out "looking" for such an occurrence.

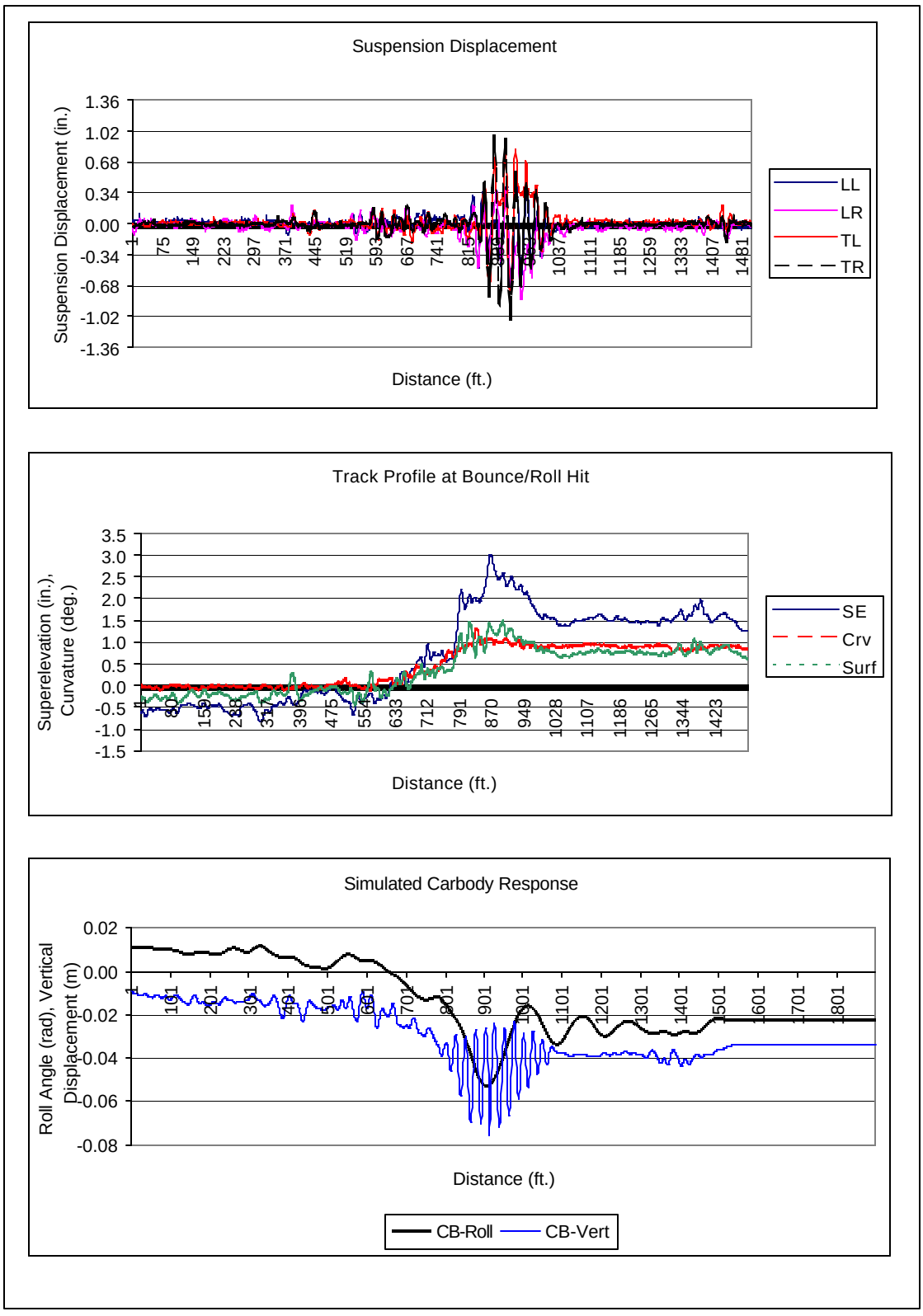

Figure 26 Suspension lift-off at a single priority-defect site

6 PREDICTOR IMPLEMENTATION

6.1 Model Attributes

The software was developed with the objective of providing a real-time performance capability for multiple cars at multiple speeds and this objective has been met. However, it is not clear that the software can be run online and integrated with the geometry computer. The ideal configuration would be to have a dedicated computer running the predictor model, with the geometry data being fed to it as they are being collected. If this is not possible, the model must be run at the end of a test segment when the geometry data file can be passed to it. In its present configuration, the model runs on a 700 MHz computer at a speed of about 6 mi. per minute. This is more than adequate to keep up with a real-time feed of data. However, it would take 20 minutes to run a 120 mi. subdivision if the data were not available until the end of the run.

6.2 Index versus Defect Interpretation

In developing its standards/regulations, the industry has sought risk/economic balance by relaxing tolerances for lower speed lines. This allows low-density lines that do not generate enough revenue to maintain a high quality infrastructure to operate trains over relatively poor quality track. The significant reduction in hit frequency when the test train was operated at 20 mph and below supports this logic.

The predictor has also been found to provide a better balance of predicted hits to false positives for Class 3 and Class 4 track than the existing measure of priority and urgent defects. However, the high frequency of hits on Class 2 track at 25 mph and the fact that none of those locations or the most significant unloading situations led to a derailment raises the question of how the predictor should be interpreted. In our opinion, it provides a basis for both an improved priority defect on Class 3 and Class 4 tracks, and an index for Class 2 track.

The present track quality index is based on measures of roughness as indicated by the standard deviation of a specific geometry measure over a length (typically 1/4 mi.) of track. The higher the standard deviation, the rougher the track and the worse the index value. Track roughness is a poor predictor of vehicle dynamic response.

We compared the effectiveness of the predictor and a track roughness measure in isolating sections of wheel unloading. The basis of comparison was the worst 100 points in a 100 mi. section of track. The track segment included the location of the worst bounce hit recorded.

Figure 27 compares the worst measured suspension activity with the worst track roughness locations. One can see that there is some correlation at mile 16 and mile 92; however, the worst measured hit at mile 21 does not register at all in the surface roughness index and the occurrences of high track roughness between mile 48 and mile 72 have no corresponding dynamic activity. Figure 28 compares the model predictions with measured suspension activity for the same track segment.

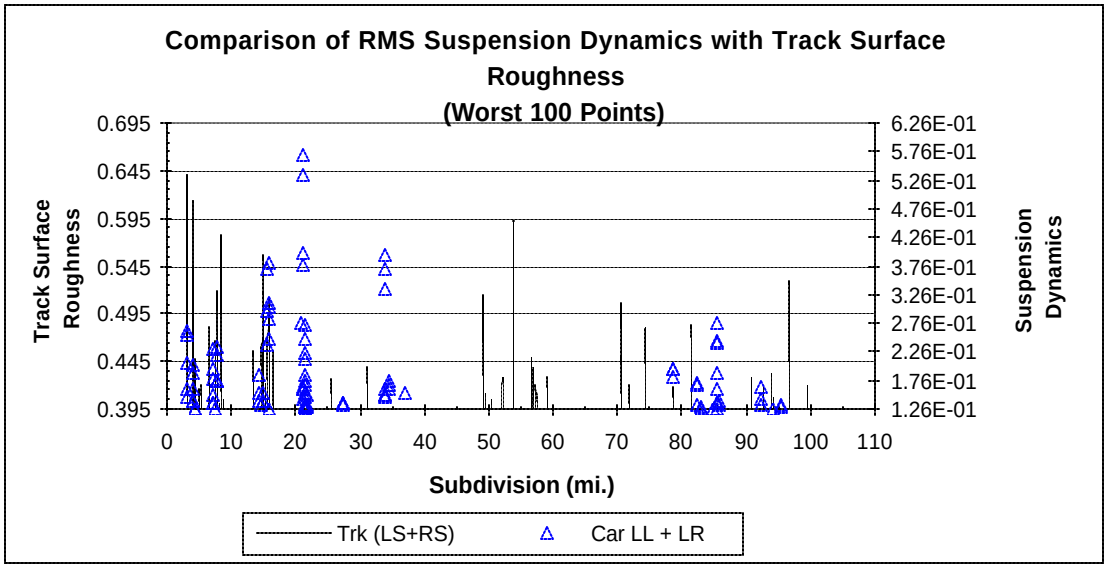

Figure 27 Comparison of measured bounce hits with track roughness

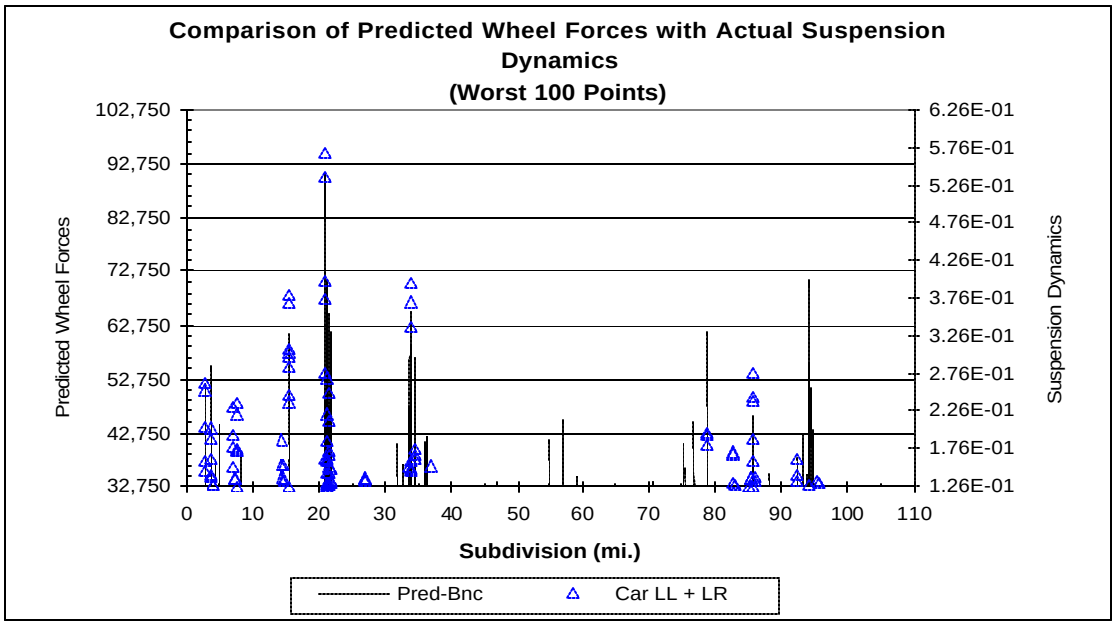

Figure 28 Comparison of predictor with measured bounce dynamics

We note that the only hits occurred at mileposts 16, 21 and 34. These three locations were in the top five predicted hit locations, whereas only one of the hits occurred in the top 100 “surface roughness” index.

Figure 29 provides an index interpretation of track quality for a Class 2 subdivision. This is the same subdivision shown in Section 4.3 to illustrate hit location sensitivity to speed (Figure 14). We note that the index consists of the predicted hit magnitudes for both the hopper car and tank car cumulated over 1/4 mi. and 1 mi. track segments. Such an interpretation is possible on this type of track because there are very few (in this case, none) 1/4 mi. segments without at least one predicted hit by either the hopper car or the tank car. If a similar output were cumulated for a Class 3 or Class 4 track, there would be many stretches with no value. If there were a desire to use the predictor as an index for the higher classes of track, the reporting threshold would have to be lowered.

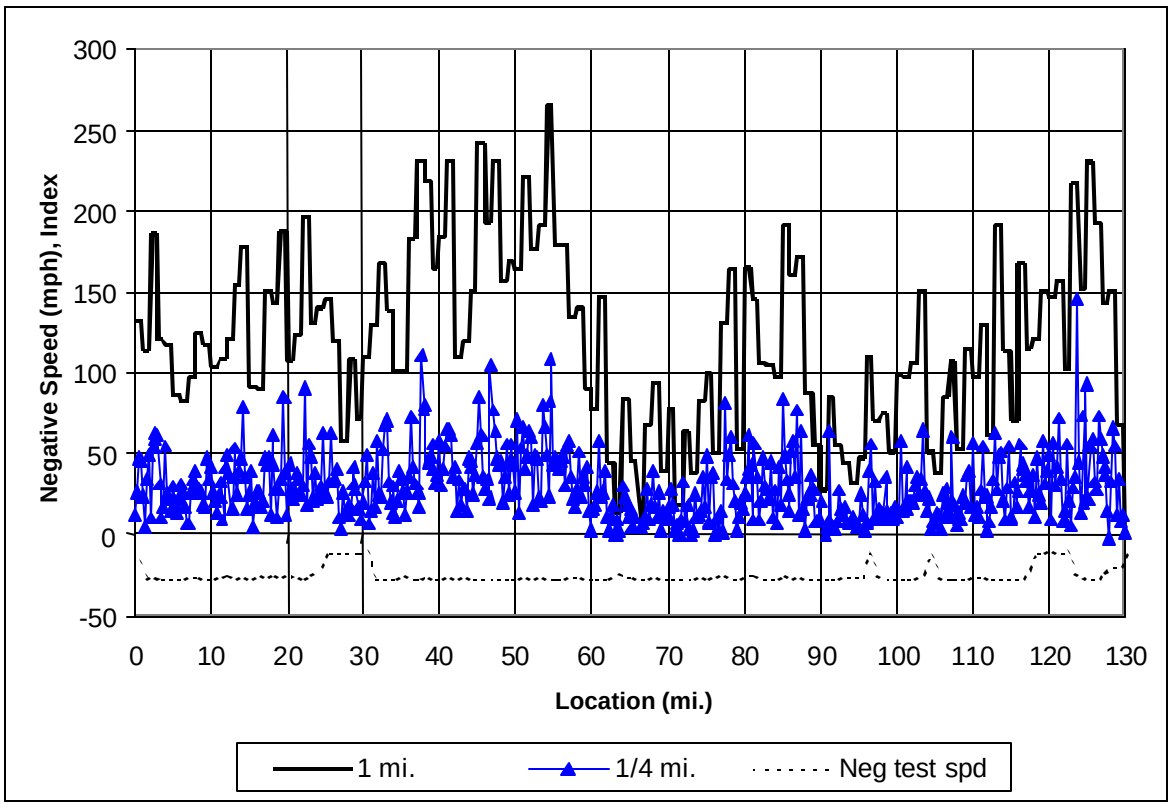

Figure 29 Index interpretation of predictor output on Class 2 track

The predictor program is currently configured as a spot problem identifier similar to regulatory defects. The model evaluates hit predictions for both hopper and tank cars at

multiple speeds. While it is possible to evaluate each car's response over its entire operating speed range, using perhaps 5 mph increments, only three representative speeds for each car type are evaluated—25, 40 and 60 mph for hopper cars and 30, 40 and 60 mph for tank cars. The lower speed for each car type has been selected to capture the most severe response for that car type, while the two higher speeds are selected to represent track class speeds. This set of base speeds is modified to reflect the actual track speed limits such that only those speeds up to and including the track speed limit are evaluated. Where a speed limit falls below one or more of these speeds, the performance is evaluated at the speed limit.

The predictor program operates by calculating the PSD content of track surface, cross-level and alignment within a "window" of data that is then input to the model for each combination of car type and speed. These are then combined with other measures to yield an index representing the severity of each car's response while operating over that track segment at each speed. The program evaluates an entire subdivision by successively advancing the "window" along the track in discrete distance intervals and calculating the response. Once calculated, the predicted response for each car type and speed is evaluated against thresholds representing base and "Priority" levels for each car/speed combination and reported when either is exceeded. In curves, the "Priority" threshold level is reduced in proportion to the curve degree to reflect the potential influence of lateral forces as discussed in subsection 2.3.3 (see Figure 6).

The output is a prediction site-unloading report. Figure 30 presents an output for a mountain subdivision with 115 mi. of mixed Class 3 and 4 track. As illustrated, the output identifies continuous track segments where one or more thresholds were exceeded and provides the maximum "index" value calculated over that segment. The reported index represents the maximum ratio of the predicted response measure to the "Priority" threshold level. Each car and speed combination found to exceed either the base or "Priority" threshold levels within the track segment is also identified using a three character mnemonic comprised of a letter—"H" for hopper or "T" for tank—and two digits for the speed of prediction. Thus, for example, the first predicted site (mile 5.201585) is a hit condition for the hopper car at 30 mph, and segment 16.84 to 16.889 involves predicted responses in excess of the priority threshold for the hopper car at 25 and 35 mph as well as for the tank car at 30 and 35 mph.

Start (mile)	End (mile)	Index	Detections	Priority Detections
5.201585	5.201585	.7557	H30	
5.745676	5.755392	.8215	H30	
8.174654	8.174654	.7805	H30	
10.924270	10.933980	1.1661		T40
11.487790	11.507230	1.1700		H40 T40
16.841290	16.889860	1.9014		H25 H35 T30 T35
18.366690	18.366690	.7751	T35	
18.794190	18.794190	1.1489		T35
19.853230	19.853230	.8282	T35	
20.096130	20.105850	.8267	T35	
21.534090	21.534090	.8719	T35	
21.602100	21.621530	1.2266	H35	T35
21.718690	21.728410	1.0141		T35
21.913010	21.913010	1.0531		T35
21.932450	21.932450	1.0962		T35
23.059500	23.059500	.7922	H25	
23.078930	23.078930	.9100	T35	
23.253810	23.302390	2.1760		H35 T30 T35
23.360690	23.360690	.7892	T35	
24.536320	24.536320	1.0334		T35
25.954850	25.954850	.7547	H25	
31.842720	31.842720	.7660	H25	
31.871870	31.871870	.7750	H25	
43.132410	43.210140	2.7175		H25 H40 H55 T30 T40 T55
44.395450	44.473180	2.7242		H25 H40 H55 T30 T40 T55
57.123120	57.152260	1.0905	H50	T50
61.747820	61.747820	1.0637		T45
66.489430	66.499150	.9326	H40 H60 T40	
77.458540	77.477970	.8370	H60 T60	
79.003340	79.032490	1.1254	H25 H40 H50	T40 T50
80.567580	80.577300	.9047	T35	
81.607170	81.636320	1.1414		T45
82.666180	82.685620	1.0302		H25
88.213900	88.213900	.7640	H25	
88.330480	88.349910	.7939	H25 H55 T55	
94.558290	94.674880	1.4297		H60 T60
94.888630	94.946920	1.2184	H25 T30	H40 H60 T40 T60
96.297410	96.316840	.8715	H25 T30 T60	
113.018200	113.144600	2.7005		H25 H40 H50 T30 T40 T50
113.290300	113.300000	.8665	H25	
113.358300	113.358300	.9260	H25	
113.416600	113.445700	.9206	H25 T50	

Total locations: 42 # Priority: 20

Figure 30 Local defect interpretation of predictor output on Class 3 and 4 track

6.3 Fixed or Variable Threshold

The present regulatory system recognizes a risk/benefit ratio by allowing lower speed lines to have larger track geometry errors than higher speed lines. If a single level of car response were applied to all track classes, either high-speed lines would see very few defects or low-speed lines would have an unrealistic number of defects. Thus, the risk relationship to traffic density and the economic impact for low-density lines (risk/cost ratio) might also be considered for the level of car unloading. This view is tied to the fact that even the most severe cases of unloading that occurred during the test program did not lead to a derailment. This could be an indication that it takes an extremely "bad" geometry condition to produce a derailment or, more likely, that a combination of bad geometry and some deterioration of car performance is required to result in a derailment. If one could link the severity of unloading more closely to derailment risk, by historic derailment analyses and/or by additional testing of hit areas with an instrumented wheel set, a better definition of a hazardous condition could be defined.

As discussed in Section 4.3, the train speed at which the data are collected has a strong influence on the number of hits recorded, and train speed is by definition related to track class. Many of the "rougher" track segments have lower speed limits and the lower speed limits coincide with the worst reaction speed for the test cars. Further investigation of other car types and application of the predictor software could help to identify an optimal set of speed limits to apply to the various track classes.

6.4 Application Notes

In the course of tracking down some high hit sites in the development stage of the predictor, a number of situations were identified that are relevant to the on-car implementation of the software. These would have to be recognized in any implementation of the software.

The first impact is the influence of reduced speed test activity. The predictor takes the recorded geometry and applies it at speeds up to and including the speed limit for that track segment. If the geometry consist slows down to pass through a switch but continues to record the track geometry, the predictor will (correctly) predict an extremely high hit when the switch is traversed at the track speed limit. This is not a reflection of the track geometry at the main (pass through) track but a reflection of taking a turn out at excessive speed. Ideally, the track geometry system should be turned off under these situations or the track speed limit should be adjusted to the switch speed at that site before the geometry data are passed through the predictor software. This situation can be

extended to temporary slow order sites. There were many sites that produced no hits when traversed at the 15 mph test speed, but that were predicted to produce significant hits when traversed at the normal 25 mph speed limit. Any test segments that are traversed at reduced speeds because of geometry-related conditions can be expected to have hits predicted if traversed at the normal track speed limit. If speed limit tables cannot be updated for each run, the user should have some method of locating switch movement and temporary slow order sites to be able to ignore the predictor results for those segments.

Another problem encountered in tracking down false hits was that of intermittent dropouts of geometry signals. There were instances in the course of the year's data where certain signals would intermittently "flatline" to zero and recover later. The steep rise in these signals can produce hits. Again, the best way to deal with these situations is to be aware of any locations where the geometry signals had dropped out. In most cases, these would be obvious when the user looks at the track profile traces at the identified hit site to assess the reason for the hit.

7 CONCLUSIONS AND RECOMMENDATIONS

7.1 Conclusions

A software program has been successfully developed that:

- can identify track geometry conditions that stimulate suspension unloading of one or both test cars,
- can identify the speed range in which the unloading will occur, and
- is more effective in locating these track geometry conditions than the present regulatory definitions of defects.

The measured data and software predictor identify more hit sites than the existing regulatory defect criteria for Class 2 tracks. Both cars, and especially the lighter hopper car, exceeded the base level threshold (67 percent-unloading) quite frequently. The frequency of "undesirable" unloading, as initially defined, is considered to be too high for it to be a reasonable surrogate of derailment risk. Nonetheless, vehicle dynamic action and suspension unloading are necessary ingredients for geometry-related derailments and the existing regulatory measures were not well correlated with the measured hit sites.

The data also suggest that vertical car dynamic action for the empty test cars is dampened in curves (i.e. it requires more stimulus in curves than in tangent track to produce the same vertical unloading). The finding is counterintuitive since most geometry-related derailments happen in curves or spirals. The data also revealed situations of unloading beyond threshold in curves that did not lead to derailment. It raises the question of what magnitude of unloading is required to pose a derailment risk.

7.2 Recommendations

The findings indicate that track geometry conditions that are missed by the present regulatory definitions can be identified. However, refinement of the definition of "undesirable" is required to reduce the number of predicted sites and better define the influence of track curvature.

We recommend further testing and analyses to refine the definition of "undesirable" unloading. More detailed insight into wheel forces is required to select a reasonable threshold and to filter out incidents of high unloading that do not pose a derailment risk (i.e. a better definition of "undesirable" unloading). The predictor software recognizes the influence of curvature with an estimated relationship of lateral wheel force with

curvature, but it is not related to measured data. To better define a threshold for an "undesirable" level of vehicle response, additional tests should be performed that would measure both suspension unloading and wheel loads (vertical and lateral) for the same test cars used to date.

We recommend a series of tests with an instrumented wheel set and suspension displacement transducers. The operating costs of the instrumented wheel set would be much higher than the previous test's instrumentation and would preclude a system-wide test. Economics dictate a controlled test program focused on specific track segments that have been previously identified as stimulating high vehicle dynamic response. The test data collected would then be analyzed to develop a correlation between the more readily measured/predicted suspension unloading and the more derailment-critical ratio of lateral-to-vertical (L/V) wheel load. The objective would be to define a set of threshold levels for vertical unloading that would vary according to the track circumstances (e.g. a more stringent threshold could be adopted in curves to recognize the role of the lateral force).

The first objective would be to develop a correlation between suspension unloading and wheel set L/V for the two empty cars used in the tests to date. It would also be desirable to extend the tests to loaded cars and possibly other car types to determine the sensitivity to vehicle characteristics. In particular, it would be desirable to assess the forces and dynamic response of a loaded car versus an empty car.

We also recommend the analysis of the data collected and of historic derailment data to assist in the interpretation of what situations pose a higher derailment risk. The existing regulatory standards allow worse geometry on low-density/low-speed lines. It would be desirable to relate the new performance-based measure to the overall risk and economics of low-density lines rather than as a fixed measure of performance.

References

Association of American Railroads, *Manual of Standards and Recommended Practices: Chapter XI, Service Worthiness Tests and Analyses for New Freight Cars*, rev. 1993.

Kortum, W. and R.S. Sharp, eds, *Multibody Computer Codes in Vehicle System Dynamics*, Supplement to Vehicle System Dynamics, Volume 22, Swets and Zeitlinger, 1992.

Roney, M.D., *Canadian Experience with FRA Track Safety Standards*, Proceedings, American Railway Engineering Association, March 1993.

TranSys Research Ltd, *Performance Measures from Track Geometry Cars: Feasibility of Wheel Load and Defect Prediction*, Transport Canada publication TP 12999E, March 1997.

Appendix A

Instrumentation

Each linear displacement transducer is a Balluff model BTL-5-E11-M0127-P-S32, providing a 4-20 mA signal proportional to measured displacements within a 0-127 mm (0-5 in.) range and has been enclosed within an aluminum housing to provide mechanical and environmental protection. Each bi-axial accelerometer is a Summit Instruments model 23203A, which measures nominally +/- 1 g along one axis and +/- 7.5 g along the other, providing a scaled voltage between 0 and 5 V proportional to the acceleration measured along each orthogonal axis.

The linear displacement transducers are actuated using a spring pre-tensioned flexible stainless steel wire whose end has been affixed to the bolster in such a way to measure the vertical relative movement between bolster and truck side frame. On the tank car installation, a linear transducer box has been rigidly mounted to each truck side frame directly above the bolster using four long threaded rods and the end of the actuating stainless steel wire has been clamped to the bolster. On the covered hopper car installation, the linear transducer boxes have been mounted on the car body and the stainless steel actuating wire has been fed to the box using a hard-shelled wire casing similar to a bicycle brake cable. Relative movement between the truck side frame and bolster are accurately detected and transmitted by having the free end of the internal wire affixed to the bolster and the free end of the hard-shell affixed to a rigid bracket mounted on the truck side frame. On both vehicles, a bi-axial accelerometer has been mounted on the bearing adapter on each side of the leading axle of one truck.

Appendix B

Parallel-Cascade Methodology

The following discussion is adapted from an article by Korenberg, et al. (2001).

To model discrete-time dynamic non-linear systems, Palm (1979) considered structures that were a finite sum of cascades of alternating dynamic linear (*L*) and static non-linear (*N*) elements. In particular, each cascade path in Palm's model consisted of a dynamic linear element followed by a logarithmic or exponential static non-linearity that was in turn followed by a dynamic linear element, so the overall model was a finite sum of *LNL* cascades.

Later, Korenberg (1982) introduced a structure that was a finite sum of *LN* elements (Figure B.1), where each static nonlinearity *N* was a polynomial. The use of polynomial non-linearities affords both theoretical and practical advantages. For example, it can be shown (Korenberg, 1991) that any causal, finite-memory, finite-order (sometimes called "doubly finite") discrete-time Volterra series can be exactly expressed as a finite sum of such *LN* polynomial cascades. In addition, a general approach called parallel cascade identification (PCI) was proposed (Korenberg, 1982, 1991) to build a parallel array approximation of a dynamic non-linear system, given only its inputs and outputs, and the use of polynomial static non-linearities in the cascades resulted in extremely rapid convergence.

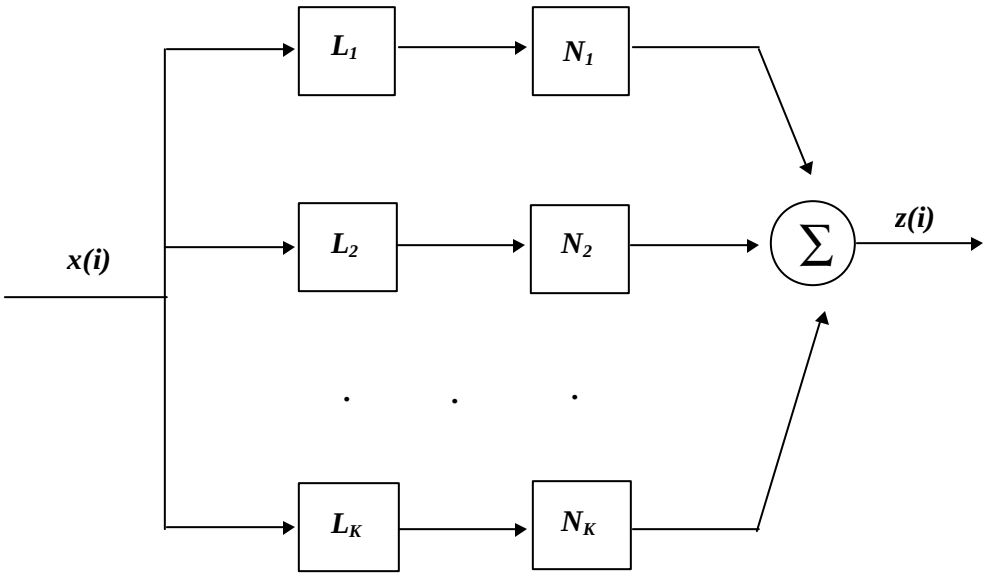

Figure B.1 Parallel-Cascade Process

In more detail, suppose that, in the single-input, single output case, $x(i),\ y(i),...,\ i = 0,...,I$, represent the input and output, respectively, of the dynamic, causal discrete-time non-linear system for which the parallel cascade approximation is to be constructed. In addition, suppose that the output $y(i)$ depends on input values $x(i), x(i-1),..., x(i-R)$, so that $(R+1)$ is the system's memory length, and let D be the assumed order of non-linearity. Then the parallel-cascade approximation to the system can be constructed as follows, where we suppose that each cascade is of *LN* structure, as in Figure B.1. The extension to cascades having further alternating *L* and *N* elements is simple (Korenberg, 1982, 1991) and is not needed for the present discussion.

A first cascade of a dynamic linear element and a polynomial static non-linearity is found to approximate the given non-linear system. In doing this, the dynamic linear element is chosen to have memory length $(R+1)$. Moreover, the polynomial of degree D is best-fit so as to minimize the mean-square error (MSE) between the system output and the polynomial's output, which is also the cascade's output. The residual—i.e., the difference between the system and the cascade outputs—is treated as the output of a new non-linear system, still having the same input. A further cascade is found to approximate the new non-linear system, a new residual is computed, and so on.

It has been shown (Korenberg, 1982, 1991) that the cascades can be selected so that any given discrete-time system having a Volterra or a Wiener series representation can be approximated to an arbitrary accuracy by a sum of the cascades. Moreover, an analogous procedure exists for creating multi-input parallel cascades, and this was used to model either the left or the right suspension displacements as output driven by both left and right rail surface inputs.

Appendix B References

Korenberg, M.J. (1982) Statistical identification of parallel cascades of linear and nonlinear systems. Proceedings 6th IFAC Symposium Ident. Sys. Param. Est. 1, 580-585.

Korenberg, M.J. (1991) Parallel cascade identification and kernel estimation for nonlinear systems. Annals of Biomedical Engineering 19, 429-455.

Palm, G. (1979) On representation and approximation of nonlinear systems. Part II: Discrete time. Biological Cybernetics 34, 49-52.

Korenberg, M.J., David, R., Hunter, I.W., Solomon, J.E. (2001) Parallel cascade identification and its application to protein family prediction. J. Biotechnology 91, 35-47.